ChemPubSoc Europe

DOI: 10.1002/chem.201600679

CHEMISTRY A European Journal Full Paper

Rhenium Complexes

A Series of Diamagnetic Pyridine Monoimine Rhenium Complexes with Different Degrees of Metal-to-Ligand Charge Transfer: Correlating ^{13}C NMR Chemical Shifts with Bond Lengths in Redox-Active Ligands

Daniel Sieh[a] and Clifford P. Kubiak*[a, b]

Abstract: A set of pyridine monoimine (PMI) rhenium(I) tricarbonyl chlorido complexes with substituents of different steric and electronic properties was synthesized and fully characterized. Spectroscopic (NMR and IR) and single-crystal X-ray diffraction analyses of these complexes showed that the redox-active PMI ligands are neutral and that the overall electronic structure is little affected by the choices of the substituent at the ligand backbone. One- and two-electron reduction products were prepared from selected starting compounds and could also be characterized by multiple spectroscopic methods and X-ray diffraction. The final product of a one-electron reduction in THF is a diamagnetic metal–metal-bonded dimer after loss of the chlorido ligand. Bond lengths in and NMR chemical shifts of the PMI ligand backbone indicate partial electron transfer to the ligand. Two-electron reduction in THF also leads to the loss of the chlorido ligand and a pentacoordinate complex is obtained. The comparison with reported bond lengths and ^{13}C NMR chemical shifts of doubly reduced free pyridine monoaldimine ligands indicates that both redox equivalents in the doubly reduced rhenium complex investigated here are located in the PMI ligand. With diamagnetic complexes varying over three formal reduction stages at the PMI ligand we were, for the first time, able to establish correlations of the ^{13}C NMR chemical shifts with the relevant bond lengths in redox-active ligands over a full redox series.

Introduction

In 1966, Jørgensen used the words "innocent" and "suspect" to describe the ambiguity in the determination of the oxidation state of the metal center in nitrosyl complexes.[1] The nitrosyl ligand can exist as NO^+, NO, NO^-, NO^{2-}, and NO^{3-} in their respective complexes and is therefore "masking" the oxidation state of the central metal atom.[2,3] Since then, the redox terms "non-innocent" and "redox-active" have been used to classify ligands that can participate in the redox chemistry of their respective complexes, even though the former term became more popular during the 1990s. These types of ligands have gained much attention in the last decades in both, basic research, as well as for their relevance in bioinorganic chemistry and catalysis, and their ability to stabilize uncommon coordination compounds, and have been reviewed recently.[3,4]

Bi- and tridentate imine- and/or pyridine-based ligands like 2,2′-bipyridines (BPY), pyridine-2,6-diimines (PDI), and diazabutadienes are among the best studied redox-active ligands and much work has been put into the experimental and theoretical exploration of the electronic structures of complexes with these ligands.[5–8] We are interested in the electrocatalytic conversion of carbon dioxide (CO_2) and have therefore studied the rhenium BPY system that was initially discovered by Lehn and others[9–11] to be a catalyst for the transformation of CO_2 to CO in great detail. A common assumption resulting from the work done by us and others[12–17] is that the catalytic activity stems from a ligand-based reduction in the catalytically active species. More specifically, it is believed that the CO_2 carbon atom binds to a singly occupied d_{z^2} orbital in a Re^0 complex having a mono-reduced BPY ligand.[14,15,18] This mechanistic assumption has recently lead to an accelerated investigation of complexes with bidentate nitrogen-based redox-active ligands for electrocatalytic CO_2 reduction.[19] We reported on molybdenum pyridine mono(ket)imine (PMI) complexes and could provide evidence that in this case the redox-active properties of the ligand were preventing rather than benefiting catalysis because of ligand–substrate C–C coupling.[20] Since then, we investigated the related rhenium complexes in more detail and will report on their reactivity with CO_2 soon. Part of this study was the isolation of reduced complexes, which will serve as

[a] Dr. D. Sieh, Prof. Dr. C. P. Kubiak
Joint Center for Artificial Photosynthesis
Division of Chemistry and Chemical Engineering
California Institute of Technology
1200 East California Boulevard
Pasadena, CA 91125 (USA)
E-mail: ckubiak@ucsd.edu

[b] Prof. Dr. C. P. Kubiak
Department of Chemistry and Biochemistry
University of California, San Diego
9500 Gilman Drive MC 0358
La Jolla, California 92093 (USA)

Supporting information for this article is available on the WWW under http://dx.doi.org/10.1002/chem.201600679.

reference points for the electro- and spectroelectrochemical studies and for stoichiometric reactions in a forthcoming publication.

We herein discuss the isolation and characterization of singly and doubly reduced Re PMI complexes along with their Re^{I} PMI^{0} parent compounds {[Re(PMI)X], X = Cl, trifuoroacetato (TFA)}. All isolated complexes are diamagnetic and allow for ^{13}C NMR spectroscopic characterization. The NMR and single-crystal X-ray investigations indicate metal-to-ligand electron transfer up to two electrons and linear correlations could be obtained by comparing the ^{13}C NMR chemical shifts of the PMI ligand with bond length alterations of the same.

Results and Discussion

Synthesis and characterization of the octahedral tricarbonyl complexes

The octahedral tricarbonyl rhenium chlorido complexes were synthesized by using the Stiddard method,[21] that is, heating an excess of the respective ligand **^{R}L** with $[Re(CO)_5Cl]$ in toluene to reflux (Scheme 1).

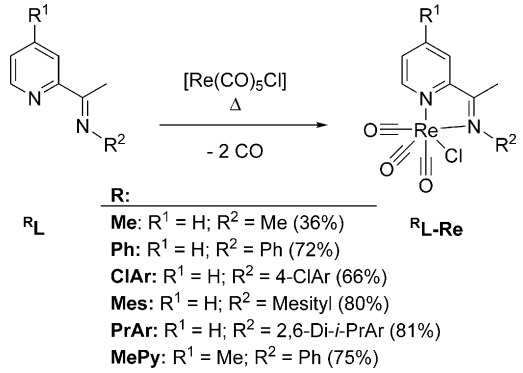

Scheme 1. Synthesis of the PMI rhenium tricarbonyl complexes with the respective yields given in brackets.

This method could be applied, even in cases where the ligand was not isolated and yielded the analytically pure, yellow/orange complexes **^{R}L-Re** in moderate to good yield after crystallization. All complexes were characterized by ^{1}H, $^{13}C\{^{1}H\}$ NMR, and IR spectroscopy, as well as single-crystal X-ray analysis. Alongside with the chlorido complexes **^{R}L-Re**, the analogue trifuoroacetato complex **^{PrAr}L-ReTFA** was investigated, which was obtained by ligand metathesis of the Cl^- ligand by using Ag(TFA).

The IR and NMR spectroscopic characterization of the neutral tricarbonyl complexes is consistent with a facial arrangement of the three carbonyl ligands. Three resonances for the carbonyl carbon atoms can be detected in the $^{13}C\{^{1}H\}$ NMR spectra for all seven complexes, two of them close to $\delta =$ 200 ppm and one slightly upfield at about $\delta = 190$ ppm (Table S1 in the Supporting Information). The close proximity of the CO resonances observed for the different complexes **^{R}L-Re** shows, that the back-bonding into the CO ligands is very little affected by the variation of the PMI ligands. The same conclusion can be made from an inspection of the three carbonyl stretching vibrations observed in the FTIR spectra. All complexes show a high energy stretching vibration at approximately $\tilde{\nu} = 2020\ cm^{-1}$ and two lower energy bands ($\tilde{\nu} \approx 1920$ and $1900\ cm^{-1}$) in acetonitrile (Table S2 in the Supporting Information, also see the Supporting Information for a comparison of data measured in MeCN or THF, and as a film). These values are very close to the related BPY complexes,[16,18] indicating a similar electronic structure. Distinct IR bands at $\tilde{\nu} =$ 1695, 1410, 1191, and $1140\ cm^{-1}$ can be observed in the IR spectrum (film) of the complex **^{PrAr}L-ReTFA**, which are absent in the spectrum of the chlorido congener. These bands are tentatively assigned to the C=O, the C–O, and the asymmetric and symmetric CF_3 stretches of the TFA ligand, respectively, based on earlier IR studies on trifluoroacetate compounds.[22]

The facial arrangement of the carbonyl ligands is also confirmed in all X-ray structures of the neutral tricarbonyl complexes **^{R}L-Re**, which are displayed in Figure 1. The very similar amount of metal-to-carbonyl-ligand back-bonding that is observed in the IR and NMR spectra is confirmed by the C≡O bond lengths in the X-ray structures, which show differences not larger than 0.013 Å between the seven complexes. The bond lengths within pyridine mono- (PMI) and diimine (PDI) ligand frameworks have previously been used to measure the amount of electron transfer from the metal center to the redox-active ligand in complexes of this kind.[6–8,23–28] Especially the imine C=N and the exocyclic C–C bonds have been found to be very diagnostic for first-row transition metals. The aforementioned bond lengths in the neutral complexes **^{R}L-Re** show only very small deviations from those of the reported crystal structure of the ligand **^{PrAr}L**[29] (Table S3 in the Supporting Information), indicating that the ligands in the octahedral Re complexes **^{R}L-Re** are in their neutral stage. Furthermore, only small differences in these bond lengths can be observed between the seven octahedral complexes showing that the modifications made only have a minor influence on the overall electronic structure. This is also indicated by the ^{13}C NMR resonances of the imine and the pyridine carbon atoms, which show differences smaller than 2 ppm.

Chemical reduction of the Re^{I} complexes

One-electron reduction

One-electron reduction was most conveniently achieved by reacting the complex **^{Mes}L-Re** with a slight excess of KC_8 in THF. After adding a chilled, yellow/orange solution of **^{Mes}L-Re** to the reductant it turned pale red quickly. Upon stirring while warming up to room temperature and finally reducing the volume of the solution in vacuum it turned dark green. ^{1}H NMR spectroscopic characterization of the raw product revealed two major products. Whereas the ^{1}H NMR shifts of the first indicates a diamagnetic species with resolved coupling patterns, the ^{1}H NMR shifts of the second one are broadened, either due to paramagnetism or a dynamic process (Figure S45 in the Supporting Information). The green, diamagnetic species, **[^{Mes}L-Re]$_2$**, could be isolated by recrystallization from a THF/pentane

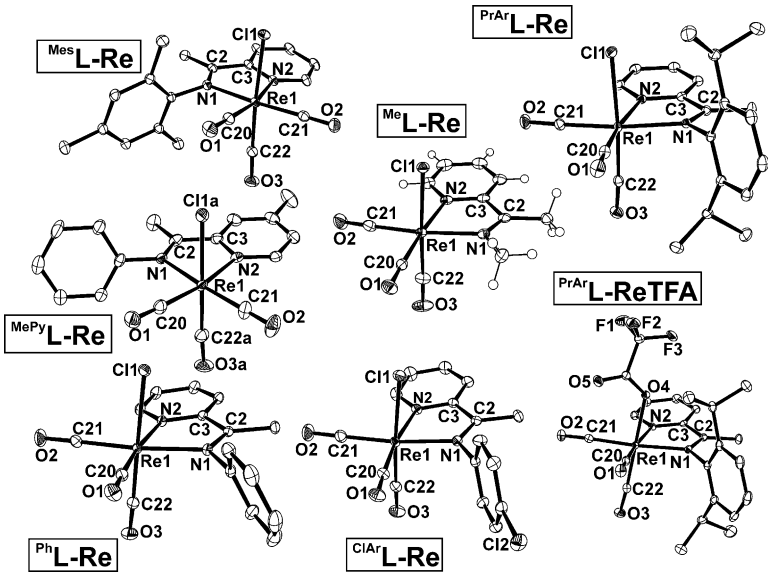

Figure 1. ORTEP representations of the molecular structures of the neutral, octahedral complexes ^{R}**L-Re** with their anisotropic displacement parameters shown at the 50% probability level. Hydrogen atoms (except for ^{Me}**L-Re**) and co-crystallized solvent molecules are omitted for clarity.

mixture at −35 °C as green crystals. The ^{1}H and ^{13}C{^{1}H} NMR spectra of this complex are consistent with an intact ligand system. Besides that, a remarkable upfield shift of some of the ^{13}C NMR resonances of the pyridine imine ligand can be observed. The imine and pyridine portion of the ^{13}C{^{1}H} NMR spectrum is displayed in Figure 2 and compared with those of ^{PrAr}**L-Re** and the doubly reduced complex ^{PrAr}**L-Re**$^{-}$. The latter one will be discussed in the next section. A comparison of the ^{1}H NMR resonances is given in Figure S59 in the Supporting Information. The carbonyl, imine, and pyridine ^{13}C NMR resonances for these complexes and ^{Mes}**L-Re** are also listed in Table 1.

By inspection of Table 1 it becomes obvious that the resonances of the two octahedral chlorido complexes ^{Mes}**L-Re** and ^{PrAr}**L-Re** are identical within the errors.

While the resonances of the pyridine 6- and 3-carbon atoms are only slightly shifted, the resonances of the imine and the other pyridine carbon atoms can be observed at significantly higher field. The imine carbon atom resonance for example is shifted 20 ppm upfield from the chlorido starting material. It should be mentioned that a strong upfield shift of these ^{13}C NMR resonances was also observed for a pyridine monoaldimine ligand that was reduced by alkali metals[28] and correla-

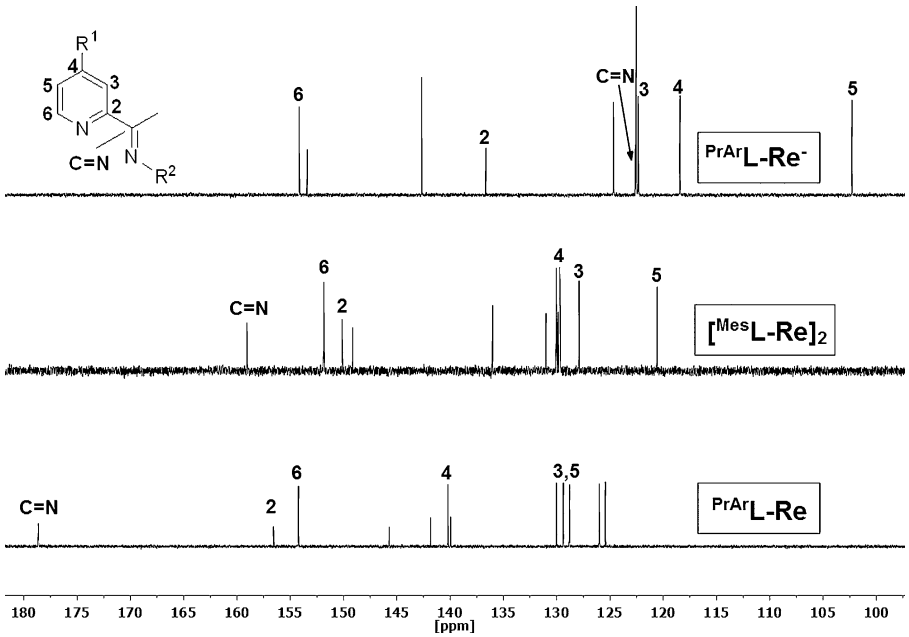

Figure 2. Portions of the ^{13}C{^{1}H} NMR spectra of ^{PrAr}**L-Re** (bottom), [^{Mes}**L-Re**]$_2$ (middle), and ^{PrAr}**L-Re**$^{-}$ (top). The resonances of the imine and pyridine carbon atoms are labeled.

Table 1. Selected $^{13}C\{^1H\}$ NMR chemical shifts in [ppm] for selected carbon atoms of the respective PMI ligand of the complexes ^{PrAr}**L-Re**, ^{Mes}**L-Re**, [^{Mes}**L-Re**]$_2$, and ^{PrAr}**L-Re**$^-$.

	^{PrAr}L-Re	^{Mes}L-Re	[^{Mes}L-Re]$_2$	^{PrAr}L-Re$^-$
C≡O	198.3	198.7	203.2	211.6
C≡O	198.0	197.9	200.6	
C≡O	189.0	189.4	190.1	
C=N	178.7	178.3	159.1	122.6
PyC(2)	156.6	156.7	150.1	136.7
PyC(3)	129.4	129.2	127.9	122.3
PyC(4)	140.2	140.3	130[a]	118.4
PyC(5)	130.0	129.8	120.6	102.3
PyC(6)	154.2	154.2	151.8	154.2

[a] The resonance of this carbon atom is nearly overlapping with the resonance of one of the aryl carbon atoms and could not be determined more precisely.

tions of ^{13}C NMR shift based on the electron transfer to the PDI ligand in Rh and Ir complexes have recently been introduced by Burger et al.[30] Furthermore, de Bruin et al. have mentioned a good agreement of the upfield shift of proton and carbon atom resonances in a pyridine aldimine Ir complex with calculated Mulliken charge densities[31] and qualitatively an upfield shift of the resonances based on an electron transfer into these kinds of ligands has been mentioned in some cases.[32] Considering this, it is reasonable to assume that the differences in the chemical shifts indicate significant electron transfer to the PMI ligand. A more detailed discussion of this is given below in comparison with the doubly reduced complex ^{PrAr}**L-Re**$^-$ (see below). The resonances of the carbonyl carbon atoms are only slightly shifted to higher frequencies (1–4 ppm, Table 1), indicating that the metal-to-CO-ligand back-bonding is not strongly increased in [^{Mes}**L-Re**]$_2$.[33,34]

By comparison with the rhenium bipyridine system, the green color of the diamagnetic complex suggests a metal–metal-bonded dimeric complex. The Re–Re dimer **[BPY-Re]$_2$** has a distinct, strong metal-to-ligand charge-transfer (MLCT) absorption band with λ_{max} at about 810 nm and less intense bands at approximately $\lambda = 605$ and 475 nm in the UV/Vis spectrum.[10,11,16,35,36] Consequently, a strong absorption at $\lambda =$ 804 nm (25 L mmol^{-1} cm) can be observed in the UV/Vis spectrum of the isolated complex [^{Mes}**L-Re**]$_2$ measured in THF (Figure S51 in the Supporting Information), which is accompanied by bands at $\lambda = 620$ (3), 517 (3), and 420 nm (15 L mmol^{-1} cm).[37] Furthermore, the IR spectrum of the complex [^{Mes}**L-Re**]$_2$ measured in a THF solution shows five C≡O stretching vibrations at $\tilde{\nu} = 1991$, 1962, 1902, 1885, and 1862 cm^{-1}. Although only four IR bands are observed for **[BPY-Re]$_2$**, the positions of the IR bands of [^{Mes}**L-Re**]$_2$ fit well with reported values for **[BPY-Re]$_2$** in THF[16,35,36] and the observation of five bands is consistent with the lower symmetry of the PMI ligand compared to BPY. For a C_2-symmetrical dimer a maximum of six IR bands can be expected based on group theory.

Single crystals suitable for X-ray diffraction were obtained from pentane diffusion into a toluene solution at −35 °C. Inspection of the molecular structure that is displayed in Figure 3 confirms the interpretation of complex [^{Mes}**L-Re**]$_2$

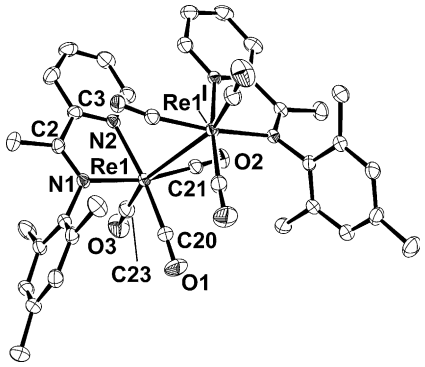

Figure 3. ORTEP representation of the molecular structure of the complex [^{Mes}**L-Re**]$_2$ with the anisotropic displacement parameters shown at the 50% probability level. Hydrogen atoms and the co-crystallized toluene molecule are omitted for clarity. Selected bond lengths [Å]: Re1–Re1^{I} 3.1397(3), Re1–N1 2.125(3), Re1–N2 2.132(3), Re1–C20 1.931(4), Re1–C21 1.930(4), Re1–C22 1.886(4), C20–O1 1.145(5), C21–O2 1.155(4), C22–O3 1.157(5), N1–C2 1.319(4), C2–C3 1.440(5).

being a metal–metal-bonded dimer with an idealized C_2 symmetry. The bond lengths within the carbonyl ligands and the pyridine imine ligand backbone as well as all Re–ligand bonds are listed in Table 2 and compared with the doubly reduced complex ^{PrAr}**L-Re**$^-$ (see below) and the octahedral starting complexes ^{R}**L-Re**. The values for the latter species are averaged over all Re^{I} starting complexes in Scheme 1 except for ^{MePy}**L-Re**. By inspection of Table 2 it becomes obvious that the statistical differences are in the range of crystallographic standard uncertainties (s.u.) of reasonable to good data sets, granting this analysis. With 3.1397(3) Å the Re–Re distance is longer by 0.06 Å than in the corresponding BPY system.[38] The higher steric demand of the PMI ligand ^{Mes}**L** compared to BPY is a tempting and probably valid explanation for this difference and the very similar HOMO–LUMO gap of approximately

Table 2. Selected bond lengths in [Å] of the complexes **L-Re**,[a] [^{Mes}**L-Re**]$_2$, and ^{PrAr}**L-Re**$^-$.

	^{R}L-Re[a]	[^{Mes}L-Re]$_2$[b]	^{PrAr}L-Re$^-$[b]
C20–O1	1.152(3)	1.145(5)	1.160(3)
C21–O2	1.150(4)	1.155(4)	1.168(2)
C22–O3	1.155(3)	1.157(5)	1.173(3)
Re1–N1	2.169(16)	2.125(3)	2.0371(15)
Re1–N2	2.170(4)	2.132(3)	2.0946(17)
Re1–C20	1.922(5)	1.931(4)	1.882(2)
Re1–C21	1.923(6)	1.930(4)	1.903(2)
Re1–C22	1.908(3)	1.886(4)	1.931(2)
C2–N1	1.294(5)	1.319(4)	1.392(2)
C2–C3	1.479(3)	1.440(5)	1.381(3)
C3–N2	1.358(2)	1.357(5)	1.409(2)
C3–C4	1.389(2)	1.402(5)	1.432(3)
C4–C5	1.390(4)	1.390(6)	1.359(3)
C5–C6	1.383(4)	1.380(6)	1.424(4)
C6–C7	1.387(3)	1.368(6)	1.357(3)
C7–N2	1.343(2)	1.364(5)	1.376(3)

[a] Averaged over all Re^{I} starting complexes ^{R}**L-Re** except for ^{MePy}**L-Re**. Standard uncertainties in brackets are based on the averaging. [b] Crystallographic s.u. in brackets.

1.53 eV compared to **[BPY-Re]$_2$** determined by UV/VIs spectroscopy indicates a similar electronic structure in solution. However, the greater metal–metal separation could also be attributed to the better electron-accepting abilities of the PMI ligand system,[39] leading to a stronger delocalization of the electron in the Re–Re bond into the backbone of the bidentate ligand and therefore to a weaker metal–metal bond.

In accordance with the small differences in the chemical shifts of the carbonyl carbon atoms comparing **[^{Mes}L-Re]$_2$** and the octahedral starting complexes **^{R}L-Re** (see above), the carbonyl C–O and the Re–$C_{carbonyl}$ bonds are not, or only slightly, affected. On the other hand, both rhenium–nitrogen bonds are shorter than in **^{R}L-Re**, indicating a stronger interaction of the PMI ligand with the metal center. The difference is small (≈0.04 Å), but the shortening is consistent with data reported for neutral and mono-reduced pyridine aldimine ligands in a series of first-row transition metal[24] and Al[27] complexes and also with a further decrease in the doubly reduced complex **^{PrAr}L-Re^{-}** (see below), indicating additional electron density in the PMI ligand compared to the complexes **^{R}L-Re**, which contain a neutral PMI ligand. Note that the bite angle of the PMI ligand only increases negligibly from approximately 74 (**^{R}L-Re**) over 74.5 (**[^{Mes}L-Re]$_2$**) to 75° (**^{PrAr}L-Re^{-}**). The bond lengths within the pyridine imine moiety, particularly the imine C2–N1 and the exocyclic C2–C3 bonds are of special interest to determine the degree of participation of the PMI ligand in the redox chemistry of the complex. Wieghardt et al. suggested a set of values for neutral, singly and doubly reduced pyridine aldimine ligands.[24,25] More importantly, besides a few known crystal structures of neutral pyridine monoaldimine (**^{R}L$_A$**)[40,41] and monoketimine (**^{R}L**)[29] ligands, a series of singly and doubly reduced pyridine aldimine ligands has been reported.[28] Comparing the bond lengths in **[^{Mes}L-Re]$_2$** with those in the unreduced complexes **^{R}L-Re**, a shortening of the imine bond (C2–N1) by 0.025 Å and an elongation of the exocyclic C2–C3 bond by 0.039 Å can be observed. Whereas the difference in the imine bond is barely larger than five times the standard uncertainty, the C–C bond is significantly longer in the reduced complex **[^{Mes}L-Re]$_2$**. Unfortunately, differences in these bond lengths up to 0.02 Å can be found within the crystal structures of different neutral pyridine aldimine ligands and the difference of these to the same bond lengths in the ketimine ligand **^{PrAr}L** is even larger (see Table S4 in the Supporting Information). A direct comparison of the bond lengths in reported reduced ligands with those in the complexes presented here is therefore not straightforward. Both, the imine C2–N1 and the exocyclic C2–C3 bond in the pyridine aldimine ligand **^{PrAr}L$_A$**[40] change by about 0.07 Å upon one-electron reduction,[28] a value very close to the one suggested by Wieghardt et al. for these kinds of ligands.[24,25] Considering this and the aforementioned perturbation of these bonds going from the complexes **^{R}L-Re** to the one-electron reduction product **[^{Mes}L-Re]$_2$**, it seems reasonable to draw two conclusions: 1) there is a significant electron transfer to the PMI ligand in **[^{Mes}L-Re]$_2$**, and 2) the added redox equivalent is not fully located on the PMI ligand.

The bond lengths within the pyridine ring are not strongly affected by the reduction. Indeed, only the C6–C7 and C7–N2 bond lengths are shortened and elongated, respectively by nearly 0.02 Å, which is within five times the s.u. of these bonds. In comparison, the singly reduced monoaldimine ligands reported by Roesky et al.[28] show bigger deviations from aromaticity (see Table S4 in the Supporting Information). This might be taken as another indication that the reduction equivalent in **[^{Mes}L-Re]$_2$** is not fully located at the PMI ligand.

It is noteworthy that for a Re,[16] but also Ru,[42] Al,[27] Ge,[43] and Ga[44] pyridine aldimine complexes, as well as a Zn pyridine ketimine complex[45] reductive C–C coupling has been observed, where two PMI ligand units are coupled through the imine carbon atom. This underscores the ligand-based redox chemistry of complexes with PMI ligands and consequently, the singly occupied molecular orbital (SOMO) in the calculated structure of the reduced chlorido complex **[^{mod}L-ReCl]$^{-}$**[46] is almost fully located at the PMI ligand (89%), with only 4% participation of the Re metal center according to Mulliken population analysis (Figure S71 in the Supporting Information, also see the Supporting Information for more information concerning the DFT calculations in this manuscript). This C–C coupling pathway upon one-electron reduction seems to be kinetically hindered for the Re pyridine ketimine complex **^{Mes}L-Re** described here. After loss of the chlorido ligand the metal participation in the SOMO is increased (Figure S73 in the Supporting Information) to 19%. This is especially apparent, when an open-shell functional like TPSS is used. The structure is more distorted towards a square pyramid (Figure S73 in the Supporting Information) compared to the more trigonal-bipyramidal structure the BP-86 functional is predicting (Figure S72 in the Supporting Information), making the molecule suitable for metal–metal bond formation.

Considering the diamagnetic nature of the dimeric complex **[^{Mes}L-Re]$_2$**, two possible scenarios arise for the increased electron density in the PMI ligands in this complex. 1) Two mostly ligand-based radicals that strongly antiferromagnetically couple (one per ^{Mes}L–Re unit) or 2) a closed-shell case, where the increased electron density at the Re center leads to strong π-back-bonding to the PMI ligand. Whereas the first one is counter intuitive considering that Re–Re radical coupling has to be assumed, the later one seems likely considering the third-row transition metal. However, it is difficult to separate these as independent effects as they are expected to influence the bond lengths and NMR shifts in the ligand backbone in a similar way.[6] DFT calculations on the dimer **[^{mod}L-Re]$_2$** as a closed-shell singlet (CSS) state converged smoothly by using either the BP-86 or the TPSS functional with comparable bonding parameters. Both methods reasonably reproduce the bond lengths observed in the X-ray structure (Table S12 in the Supporting Information), but slightly underestimate the strength of the Re–Re bond. Broken symmetry calculations starting from a converged triplet wavefunction converged to singlet structures, indicating that the DFT level of theory does predict a closed-shell singlet ground state. The DFT-calculated HOMO of the CSS dimer **[^{mod}L-Re]$_2$** is completely delocalized (Figure S78 in the Supporting Information) with the largest portion (52% according to Mulliken population analysis) being located at the two PMI ligands. A smaller fraction (16%) is located at

the six CO ligands, leaving 16% participation of each of the two Re centers.

Dissolution of the isolated, green dimer in MeCN leads to a color change to yellow/orange. By inspection of the IR spectrum of the complex recorded in MeCN, two bands can be detected at $\tilde{\nu}=2009$ and 1897 cm^{-1}. The low energy band is broad and probably consists of two overlapped bands. These bands are very close to those reported for a pyridine aldimine rhenium tricarbonyl butyronitrile radical[16] and some related bipyridine complexes[13,47] generated in spectroelectrochemical experiments and it seems likely that the dimeric complex **[^{Mes}L-Re]$_2$** breaks up in more strongly coordinating solvents, like MeCN, to form the solvated radical **^{Mes}L-Re(NCMe)$^{\bullet}$**.

Two-electron reduction

Two-electron reduction was performed by using an excess of sodium amalgam (Na/Hg) for the complexes **^{Ph}L-Re**, **^{PrAr}L-Re**, and **^{PrAr}L-ReTFA** in THF (Scheme 2). Reduction with an excess of KC_8 was also successfully applied for ^{PrAr}L-Re, but was found to be less reliable for the preparation of clean **^{R}L-Re^{-}**.

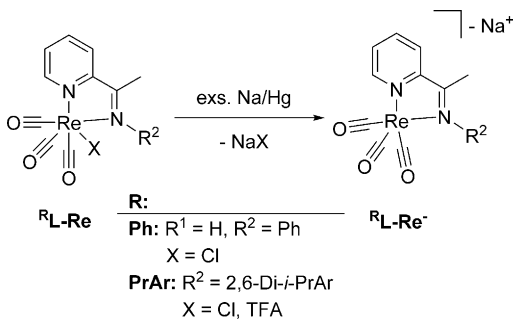

Scheme 2. Two-electron chemical reduction of the complexes **^{Ph}L-Re**, **^{PrAr}L-Re**, and **^{PrAr}L-ReTFA** with Na/Hg.

Reduction of the complexes **^{Ph}L-Re** and **^{PrAr}L-Re** with an excess of Na/Hg in THF resulted in a color change to deep red. Inspection of the reaction products by NMR spectroscopy indicated the clean formation of a single, diamagnetic product. All proton resonances of the pyridine hydrogen atoms are observed upfield from their counterparts in the respective starting materials **^{R}L-Re** (see Figure S60 in the Supporting Information for a comparison for **^{PrAr}L-Re**). Furthermore, inspection of the ^{1}H and $^{13}C\{^1H\}$ NMR spectra indicate a higher symmetry than in the octahedral complexes **^{R}L-Re**. For example, only one set of signals is observable for the isopropyl groups in **^{PrAr}L-Re^{-}**. Consistent with this, only one resonance for the carbonyl carbon atoms can be observed at $\delta=211.6$ ppm in the $^{13}C\{^1H\}$ NMR spectra of the reduction products, indicating 1) slightly higher back-bonding into the carbonyl ligands and 2) the loss of the chlorido ligand and the fast exchange of the three carbonyl ligands.[33,34] The ^{13}C NMR resonances of the imine and all pyridine carbon atoms except that of the C6 atom are shifted upfield compared to those of the starting complexes **^{R}L-Re** and a clear trend is visible going from **^{R}L-Re** over **[^{Mes}L-Re]$_2$** to **^{R}L-Re^{-}** (Figure 2 and Table 1). The chemical shifts observed for these carbon atoms are very similar in both reduction products **^{Ph}L-Re^{-}** and **^{PrAr}L-Re^{-}** and also reasonably similar to the previously reported complex **^{PrAr}L-Mo^{2-}**.[20]

Reduction of the TFA complex **^{PrAr}L-ReTFA** with Na/Hg results in the formation of **^{PrAr}L-Re^{-}**, the same product that was obtained from the analogous chlorido complex **^{PrAr}L-Re** as confirmed by ^{1}H NMR spectroscopy (see Figure S61 in the Supporting Information). The isolated dimer could also be further reduced with a slight excess of KC_8, resulting in a red species with similar ^{1}H NMR chemical shifts for the pyridine protons as observed for **^{Ph}L-Re^{-}** and **^{PrAr}L-Re^{-}** (Figure S62 in the Supporting Information). However, the reaction proceeded less cleanly than the reductions with excess Na/Hg starting from the chlorido complexes **^{R}L-Re** and we did not attempt to isolate the reduced complex **^{Mes}L-Re^{-}** this way. The complex **^{Ph}L-Re^{-}** was only prepared in situ in this study and characterized by NMR and IR spectroscopy, but the complex **^{PrAr}L-Re^{-}** was isolated and further characterized by single-crystal X-ray diffraction and elemental analysis. Three C≡O stretching vibrations can be observed in the IR spectrum of the complex **^{PrAr}L-Re^{-}**, which are located at $\tilde{\nu}=1951$, 1844, and 1835 cm^{-1} (in MeCN solution) and are shifted to lower energies by 60–80 wavenumbers relative to the starting material, indicating higher back-bonding into the carbonyl ligands. These bands compare well with those observed for the **BPY-Re^{-}** complexes.[16,17,36,38]

Single crystals suitable for X-ray diffraction of the doubly reduced complex **^{PrAr}L-Re^{-}** were obtained from a very dilute pentane solution that contained small amounts of THF at −35 °C. The asymmetric unit contains one complex molecule and two half sodium atoms. One sodium atom bridges two complex molecules and is coordinated by two carbonyl ligands and four THF molecules. The second Na atom is coordinated by six THF molecules. Part of the asymmetric unit is displayed in Figure 4.[48]

The Re metal center in the molecular structure of **^{PrAr}L-Re^{-}** displays a pseudo-trigonal-bipyramidal coordination geometry with the trigonal plane spanned by the N1, C21, and C22 atoms ($\Sigma\measuredangle=360°$) and a distortion towards a Y-shape (C21-

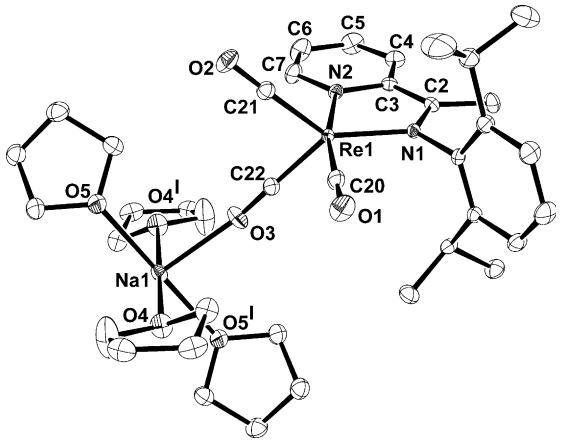

Figure 4. ORTEP representation of the molecular structure of the complex **^{PrAr}L-Re^{-}** with the anisotropic displacement parameters shown at the 50% probability level. Hydrogen atoms and the half $Na(THF)_6$ molecule are omitted for clarity.

Re1-C22 86.94(9)°) can be observed. Selected bond lengths are listed in Table 2. A direct comparison of the bond lengths to and within the carbonyl ligands to those in the complexes ^{R}**L-Re** and [^{Mes}**L-Re**]$_2$ is not fully valid because of the different coordination environment and the coordination of the sodium atom in the solid-state structure. Least affected by these changes is the carbonyl ligand C20–O1 bond *trans* to the pyridine nitrogen atom. This ligand shows some shortening of the Re1–C20 bond (0.04 Å), but only a very small, insignificant elongation of the C20–O1 bond (< 0.01 Å). The rhenium–nitrogen bond lengths Re1–N1 and Re1–N2 are further decreased going from ^{R}**L-Re** over [^{Mes}**L-Re**]$_2$ to ^{PrAr}**L-Re**$^{-}$ showing a stronger interaction of the central metal atom with the PMI ligand. The bonds within the pyridine imine moiety show significant deviations from the octahedral complexes ^{R}**L-Re**. Most noticeably, the imine C2–N1 and the exocyclic C2–C3 bonds are elongated and shortened by 0.1 Å, respectively, indicating a significant electron transfer to the PMI ligand. Although Wieghardt et al. predict an elongation of the C–N bond by 0.2 Å for a doubly reduced pyridine aldimine ligand, the observed shortening of the C–C bond in the complex ^{PrAr}**L-Re**$^{-}$ is very close to the predicted value.[24,25] The absolute values are different, however. Furthermore, distortions of 0.15 (C–N) and 0.10 Å (C–C) were observed in the solid-state structure of the free pyridine aldimine ligand ^{PrAr}**L**$_A$ upon two-electron reduction.[28] The larger distortion of the C–N bond might also be attributed to sodium coordination to this bond observed in the solid-state structure. The bond lengths within the pyridine ring in the crystal structure of the complex ^{PrAr}**L-Re**$^{-}$ are significantly different from the complexes ^{R}**L-Re** (Table 2) and the expected values for an aromatic system.[49] In fact, they are much closer to what is expected[49] for alternating sp^2–sp^2 single and double bonds (Table 2 and Figure 5). This deviation is less pronounced in the doubly reduced ligand ^{PrAr}**L**$_A$,[28] but again, sodium coordination to these bonds might introduce some artifacts.

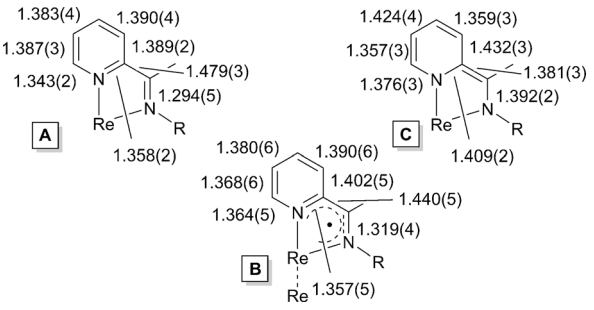

Figure 5. Comparison of the bond lengths in [Å] within the pyridine imine moiety of the complexes A) ^{R}**L-Re**, B) [^{Mes}**L-Re**]$_2$, and C) ^{PrAr}**L-Re**$^{-}$.

Correlation of the ^{13}C NMR shifts with the X-ray bond parameters

As shown above, both, the ^{13}C NMR data as well as the bond matrices derived from the single-crystal X-ray data indicate an increasing amount of electron transfer to the PMI ligand starting with the complexes ^{R}**L-Re** over [^{Mes}**L-Re**]$_2$ to ^{PrAr}**L-Re**$^{-}$. A summary of the conclusions that can be drawn from the crystal-structure data is depicted in Figure 5.

The bond lengths in the octahedral complexes ^{R}**L-Re** (structure A in Figure 5) are only slightly different from those observed in the crystal structure of the free ligand ^{PrAr}**L**[29] and the PMI ligands in these complexes can be interpreted as essentially neutral. In the dimeric complex [^{Mes}**L-Re**]$_2$ (structure B in Figure 5) obtained by one-electron reduction, the C=N and the exocyclic C–C bonds are both distorted towards a ligand-based radical. The DFT calculations presented above, however, indicate a closed-shell singlet state with a fully delocalized HOMO. Therefore, the radical dot in Figure 5 should not imply a radical, but there is formally one electron delocalized per RePMI unit between the metal center and the ligand. Most of the bonds within the pyridine ring are not very different from the unreduced complexes ^{R}**L-Re**. Finally, in the doubly reduced complex ^{PrAr}**L-Re**$^{-}$ (structure C in Figure 5), the former imine C–N bond is elongated to a C(sp^2)–N single bond and the exocyclic C–C bond is closer to a C(sp^2)–C(sp^2) double bond than a single bond and the aromaticity in the pyridine ring is broken. This interpretation is widely used for pyridine diimine complexes and has also been used for some pyridine monoimine complexes.[23–25,27,50] The development of these bond lengths and the Re–N distances are reasonably reproduced in the DFT-optimized structures (Tables S14 and S15 in the Supporting Information).

Burger et al. were the first one to introduce the use of ^{13}C NMR data to measure the amount of metal-to-ligand electron transfer in redox-active PDI ligands and showed good correlations of carbon NMR shifts with Hammett parameter and experimental and theoretical bond lengths in square-planar Rh and Ir PDI complexes.[30] With a series of diamagnetic complexes varying over three formal reduction stages at the PMI ligand we are able to correlate the ^{13}C NMR shifts with bond alterations over a wider range. Examples of these correlations are given in Figure 6 (see Figures S64 and S65 in the Supporting Information for more correlations). Excellent linear correlations were obtained for the ^{13}C NMR shifts of the imine carbon atom and the one in the pyridine 2-position with the respective bonds these two carbon atoms are involved in except for the C–N_{py} bond. A gradual and smooth transition from a C=N to a C(sp^2)–N and a C(ar)–C(sp^2) to a C(sp^2)=C(sp^2) (for C2–C3 or C(sp^2)–C(sp^2) in the case of C3–C4) bond can be observed, respectively, in both, the X-ray and the NMR data. Similarly good correlations were obtained when the DFT-computed bond lengths were used instead of the experimentally observed ones (Figures S66 and S67 in the Supporting Information). Correlations of the ^{13}C NMR shifts of the other carbon atoms in the pyridine ring with the bond lengths of the bonds these atoms are involved in mostly did not give linear relationships. However, the shift of the carbon atom in the pyridine 4-position could be correlated with the C=N and the exocyclic C–C bond lengths (Figure S65 in the Supporting Information). It is important to mention that the free ligand is not necessarily a reference point in this analysis and no linear correlations are obtained when its chemical shifts and bond lengths were

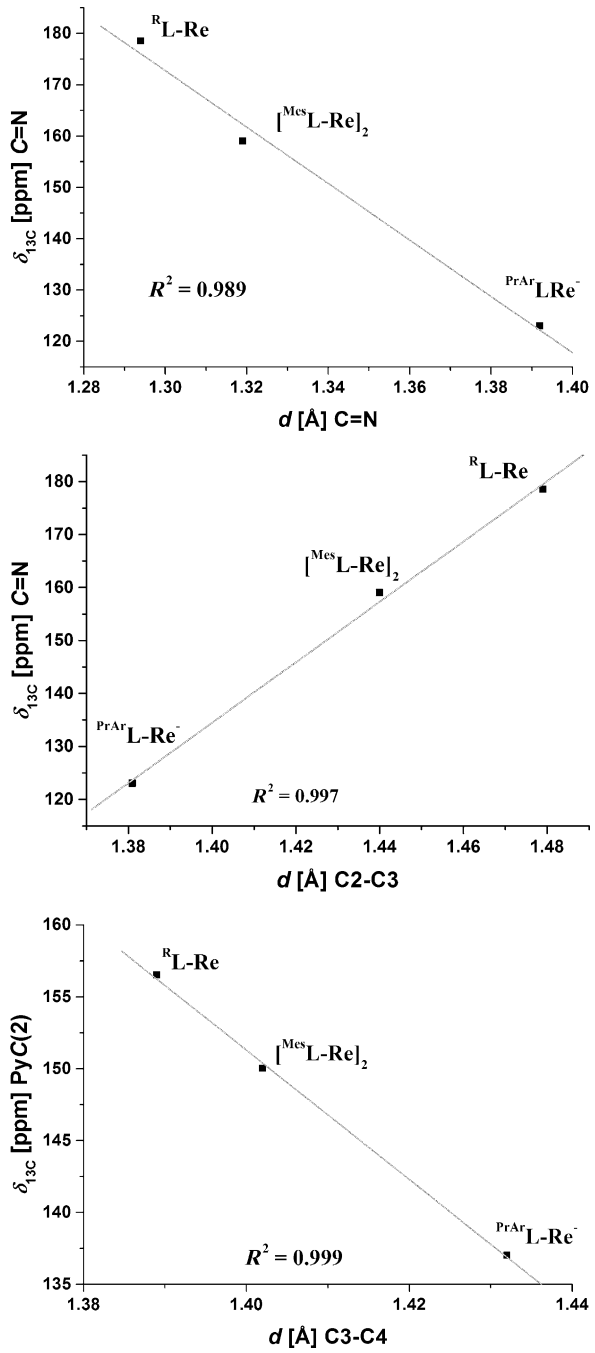

Figure 6. Correlation of the ^{13}C NMR shifts of the complexes ^{R}**L-Re**, [^{Mes}**L-Re**]$_2$, and ^{PrAr}**L-Re**$^-$ with the bond lengths observed in the corresponding X-ray structures.

included in the correlations shown above. For example, although the ^{13}C NMR resonance of the carbon atom in the 2-position stays unaffected, the one for the imine carbon atom is shifted downfield by 10 ppm upon coordination. Coordination obviously can change the shielding of the carbon atoms significantly, even if the bond lengths are not affected and the ligand is considered to be in its neutral state.

No quantification of the amount of electron transfer to the PMI ligand can be made purely based on the correlations presented above. An estimate can be obtained by comparison with the doubly reduced free pyridine aldimine ligand $^{PrAr}L_A^{2-}$ reported by Roesky et al.,[28] however. The authors reported an upfield shift of 54 ppm for the imine carbon atom and of 21 ppm for the one in the pyridine 2-position. These values are (almost) identical with the differences observed for the two-electron reductions of the complexes ^{Ph}**L-Re** and ^{PrAr}**L-Re**. The values for the other pyridine carbon atoms in the rhenium complexes do not match the ones in the free ligands that exactly, but the trend is nicely reflected (Tables 1 and S5 in the Supporting Information). Assuming that the alkali metals in the reduced free ligand $^{PrAr}L_A^{2-}$ are separated by the moderately coordinating solvent (i.e., [D_8]THF) and the NMR chemical shifts observed are therefore really of a free ligand, an upfield shift of about 50–55 ppm (C=N) and 20 ppm (PyC(2)) would correspond to two redox equivalents located on the PMI ligand.

Conclusion

We have investigated a series of rhenium pyridine ketimine complexes, which are closely related to the famous rhenium bipyridine CO_2 reduction catalyst. The CO_2 reduction properties of these complexes are going to be reported in a subsequent publication. One- and two-electron reduction products obtained from these complexes indicate an increasing amount of electron transfer to the PMI ligand. Perturbations in the bond lengths of the PMI and PDI ligand frameworks have been used for more than a decade to measure the amount of ligand reduction. Correlations of the ^{13}C NMR chemical shifts of relevant carbon atoms in the PMI ligands of the complexes studied here with the bond lengths observed in their crystal structures show excellent linear dependencies. Together with the recent report of Burger et al. this provides a new tool to measure the amount of ligand reduction in redox-active ligands.

Experimental Section

General: Even though we did not observe water or air sensitivity of the octahedral chlorido complexes, manipulations of all complexes were performed by using standard Schlenk techniques or in a dinitrogen-filled glovebox if not otherwise stated. ^{1}H, ^{13}C{^{1}H}, and ^{19}F NMR spectra were recorded on Varian 400 or 200 MHz or a 400 MHz Bruker NMR spectrometer equipped with a cryoprobe. ^{1}H and ^{13}C NMR signals were referenced to the residual solvent signals and are given relative to $(CH_3)_4Si$. ^{19}F NMR signals were referenced against CCl_3F. The assignments of the ^{1}H and ^{13}C NMR signals were carried out by combined analyses of 1D and ^{1}H,^{1}H and ^{1}H,^{13}C correlated 2D spectra (^{1}H,^{1}H COSY, HSQC, HMBC, and ADEQUATE as needed). Signals of higher order are reported as first-order signals whenever the coupling constants could reasonably be determined. Diffusion coefficients were determined by DOSY spectroscopy on a 500 MHz Varian NMR spectrometer. Infrared spectra were recorded as thin films on an ATR cell or as MeCN or THF solutions with a resolution of 4 cm^{-1} on a Thermo Scientific Nicolet iS5 FTIR spectrometer. IR peaks are given relative to each other as: s = strong, m = medium, w = weak, vw = very weak, or sh = shoulder. Microanalyses were performed by the Midwest Microlab, LLC. The ligands ^{Ph}**L**[20] and ^{PrAr}**L**[20,51] were synthesized according to literature procedures. Air- and water-free non-deuterat-

ed solvents were obtained from a commercial solvent purification system. CD_2Cl_2 was used as received as 1 g ampoules, which were opened in a N_2-filled glovebox. THF and [D_8]THF used for the reductions were additionally stirred over Na, filtered, and stored over sieves in a dinitrogen-filled glovebox prior to use. KC_8 was prepared by using a literature procedure.[52] All other reagents were purchased from commercial sources and used as received.

X-ray crystallography: Crystals of the complexes suitable for X-ray structural determinations were mounted in polybutene oil on a glass fibre and transferred on the goniometer head to the precooled instrument. Crystallographic measurements were carried out with $Mo_{K\alpha}$ radiation on a Bruker APEXII or a D8 VENTURE single-crystal diffractometer. Data were integrated by using SAINT[53] and a numerical and multi-scan absorption correction was applied with the program SADABS.[54] The structures were solved by direct methods by using SHELXS[55] or SIR92[56] and refined against F^2 by full-matrix least-squares by using SHELX97[55] and/or ShelXle[57] by using all unique data. All non-hydrogen atoms were anisotropically refined unless otherwise reported; the hydrogen atoms were placed on geometrically calculated positions and refined by using a riding model. More details of the data collection and refinement are given in the Supporting Information and the supplemental cif files.

Analytical data of ^{PrAr}L: ^{1}H NMR ([D_8]THF, 400 MHz): $\delta = 8.62$ (ddd, 1H; $^3J = 4.8$, $^4J = 1.8$, $^5J = 1.0$ Hz, PyH(6)), 8.36 (ddd, 1H; $^3J = 8.0$, $^4J = 1.1$, $^5J = 1.1$ Hz, PyH(3)), 7.83 (ddd, 1H; $^3J = 7.9$,, $^3J = 7.5$, $^4J = 1.8$ Hz, PyH(4)), 7.40 (ddd, 1H; $^3J = 7.5$, $^3J = 4.8$, $^4J = 1.2$ Hz, PyH(5)), 7.13 (m, 2H; ArH(3,5)), 7.13 (m, 1H; ArH(4)), 2.75 (sept, 2H; $^3J = 6.9$ Hz, $CH(CH_3)_2$), 2.17 (s, 3H; $NCCH_3$), 1.14 (d, 6H; $^3J = 6.9$ Hz, $CH(CH_3)_2$), 1.11 ppm (d, 6H; $^3J = 6.9$ Hz, $CH(CH_3)_2$); ^{13}C{^{1}H} NMR ([D_8]THF, 100 MHz): $\delta = 168.1$ ($NCCH_3$), 157.4 (PyC(2)), 149.7 (PyC(6)), 147.8 (ArC(1)), 136.4 (ArC(2,6)), 137.2 (PyC(4)), 125.8 (PyC(5)), 121.8 (PyC(3)), 124.5 (ArC(4)), 123.8 (ArC(3,5)), 29.3 ($CH(CH_3)_2$), 23.8, 23.2 ($2\times CH(CH_3)_2$), 17.4 ppm ($NCCH_3$).

Preparation of ^{Me}L: An oven-dried Schlenk flask was charged with dry CH_2Cl_2 (20 mL). Methylammonium chloride (300 mg, 4.44 mmol), triethylamine (0.93 mL, 0.67 g, 6.6 mmol), 2-acetylpyridine (0.5 mL, 0.5 g, 4 mmol), and several spatulas of Na_2SO_4 were added against a dinitrogen stream. Dry methanol (10 mL) was added and the reaction mixture was stirred at RT. Over the course of two days more methylammonium chloride (556 mg, 8.23 mmol) and triethylamine (1.61 mL, 1.17 g, 11.7 mmol) were added in four portions while the reaction was stirred at RT. The reaction mixture was then filtered and the solvent was removed in vacuum. The residue was extracted with benzene (30 mL), filtered, and the benzene phase was washed two times with deionized water (5 mL). After being dried over Na_2SO_4, the benzene was removed in vacuum, yielding 69 mg of the raw ligand ^{Me}L, which was used without further purification for the complexation reaction.

Synthesis of ^{Me}L-Re: The raw ligand ^{Me}L (69 mg, max. 0.51 mmol) was dissolved in toluene (1 mL) and combined with [$Re(CO)_5Cl$] (130 mg, 0.36 mmol) suspended in toluene (5 mL) in a 100 mL Schlenk flask. The reaction mixture was heated to reflux for 22.5 h. After being cooled to RT, the solvent was removed in vacuum and the residue was co-evaporated with pentane (2 mL). The yellow solid was the washed four times with pentane (1.5 mL), followed by two times with Et_2O (1 mL). The raw product was then recrystallized from pentane diffusion into a CH_2CL_2 solution, which yielded 55 mg (0.13 mmol, 36%) of the complex ^{Me}L-Re as well as single crystals suitable for X-ray diffraction. ^{1}H NMR ([D_8]THF, 400 MHz): $\delta = 9.01$ (ddd, 1H; $^3J = 5.4$, $^4J = 1.4$, $^5J = 0.9$ Hz, PyH(6)), 8.23–8.16 (m, 2H; PyH(3), PyH(4)), 7.68 (ddd, 1H; $^3J = 7.3$, $^3J = 5.4$, $^4J = 2.0$ Hz, PyH(5)), 3.96 (q, 3H; $^5J = 1.0$ Hz, NCH_3), 2.59 ppm (q, 3H; $^5J = 1.0$ Hz, $NCCH_3$); ^{13}C{^{1}H} NMR ([D_8]THF, 100 MHz): $\delta = 199.7$ (C≡O), 199.0 (C≡O), 189.2 (C≡O), 175.0 ($NCCH_3$), 157.7 (PyC(2)), 154.0 (PyC(6)), 140.2 (PyC(4)), 129.0 (PyC(5)), 128.1 (PyC(3)), 47.5 (NCH_3), 16.1 ppm ($NCCH_3$); IR (THF): $\tilde{\nu} = 2018$ (s, C≡O), 1916 (s, C≡O), 1892 cm^{-1} (s, C≡O); IR (MeCN): $\tilde{\nu} = 2021$ (s, C≡O), 1915 (s, C≡O), 1898 cm^{-1} (s, C≡O); IR (film): $\tilde{\nu} = 3078$ (vw), 2980 (vw), 2933 (vw), 2869 (vw), 2013 (s, C≡O), 1898 (sh, C≡O), 1878 (s, C≡O), 1680 (vw), 1626 (vw), 1600 (w), 1565 (vw), 1478 (w), 1443 (w), 1425 (sh), 1378 (w), 1325 (w), 1302 (w), 1257 (w), 1182 (vw), 1166 (w), 1141 (vw), 1099 (vw), 1066 (w), 1027 (vw), 969 (vw), 940 (vw), 907 (w), 778 (w), 752 (w), 646 (w), 630 (w), 610 (vw), 591 cm^{-1} (w); elemental analysis calcd (%) for $C_{11}H_{10}ClN_2O_3Re$: C 30.04, H 2.29, N 6.37; found: C 30.28, H 2.35, N 6.40.

Synthesis of ^{Ph}L-Re: The ligand ^{Ph}L (85 mg; 0.43 mmol) was dissolved in toluene (1 mL) and combined with [$Re(CO)_5Cl$] (104 mg, 0.29 mmol) suspended in toluene (6 mL) in a 100 mL Schlenk flask in a N_2-filled glovebox. The flask was taken out of the box and equipped with a reflux condenser under a dinitrogen atmosphere. The suspension was heated to reflux under N_2 for 13.5 h. An orange solid formed during this time. The reaction mixture was allowed to cool to RT and was then filtered in a N_2-filled glovebox. The orange solid was washed five times with toluene (1 mL) and then dried in vacuum. The raw product was then recrystallized by pentane diffusion into a $CHCl_3$ solution leading to 105 mg (0.21 mmol, 72%) of the yellow/orange, crystalline product ^{Ph}L-Re as well as single crystals suitable for X-ray diffraction, which were washed three times with a mixture of pentane/$CHCl_3$ (3:1, 5 mL) and dried in vacuum. ^{1}H NMR (CD_2Cl_2, 400 MHz): $\delta = 9.06$ (ddd, 1H; $^3J = 5.4$, $^4J = 1.6$, $^5J = 0.8$ Hz, PyH(6)), 8.16 (ddd, 1H; $^3J = 7.9$, $^3J = 7.8$, $^4J = 1.6$ Hz, PyH(4)), 8.06 (ddd, 1H; $^3J = 8.1$, $^4J = 1.4$, $^5J = 0.8$ Hz, PyH(3)), 7.68 (ddd, 1H; $^3J = 7.7$, $^3J = 5.4$, $^4J = 1.4$ Hz, PyH(5)), 7.54 (m, 2H; ArH(3), ArH(5)), 7.41–7.30 (m, 2H; ArH(4), ArH(2or6)), 7.09 (m, 1H; ArH(2or6)), 2.43 ppm (s, 3H; $NCCH_3$); ^{13}C{^{1}H} NMR (CD_2Cl_2, 100 MHz): $\delta = 199.0$ (C≡O), 196.6 (C≡O), 188.1 (C≡O), 175.1 ($NCCH_3$), 156.4 (PyC(2)), 153.8 (PyC(6)), 150.0 (ArC(1)), 139.8 (PyC(4)), 130.3 (br, ArC(3or5)), 130.1 (br, ArC(3or5)), 129.4 (PyC(5)), 128.2 (PyC(3)), 128.0 (ArC(4)), 122.0 (br, ArC(2or6)), 120.9 (br, ArC(2or6)), 18.8 ppm ($NCCH_3$); ^{1}H NMR ([D_8]THF, 400 MHz): $\delta = 9.07$ (ddd, 1H; $^3J = 5.4$, $^4J = 1.5$, $^5J = 0.8$ Hz, PyH(6)), 8.30 (ddd, 1H; $^3J = 8.0$, $^4J = 1.5$, $^5J = 0.8$ Hz, PyH(3)), 8.23 (ddd, 1H; $^3J = 7.9$, $^3J = 7.6$, $^4J = 1.5$ Hz, PyH(4)), 7.74 (ddd, 1H; $^3J = 7.5$, $^3J = 5.4$, $^4J = 1.4$ Hz, PyH(5)), 7.51 (m, 2H; ArH(3), ArH(5)), 7.44 (m, 1H; ArH(2or6)), 7.33 (m, 1H; ArH(4)), 7.08 (m, 1H; ArH(2or6)), 2.44 ppm (s, 3H; $NCCH_3$); ^{13}C{^{1}H} NMR ([D_8]THF, 100 MHz): $\delta = 199.9$ (C≡O), 197.4 (C≡O), 188.9 (C≡O), 176.3 ($NCCH_3$), 157.2 (PyC(2)), 154.3 (PyC(6)), 151.1 (ArC(1)), 140.1 (PyC(4)), 130.5 (br, ArC(3or5)), 130.3 (br, ArC(3or5)), 129.8 (PyC(5)), 129.2 (PyC(3)), 128.1 (Ar**C**(4)), 123.0 (br, ArC(2or6)), 121.4 (br, ArC(2or6)) and 18.3 ppm ($NCCH_3$); diffusion coefficient ([D_3]MeCN, DOSY): $D_0 = 16.5\times10^{-10}$ m^{2}s^{-1}; IR (THF): $\tilde{\nu} = 2021$ (s, C≡O), 1923 (s, C≡O), 1893 cm^{-1} (s, C≡O); IR (MeCN): $\tilde{\nu} = 2022$ (s, C≡O), 1919 (s, C≡O), 1899 cm^{-1} (s, C≡O); IR (film): $\tilde{\nu} = 2982$ (w), 2869 (w), 2017 (s, C≡O), 1908 (s, C≡O), 1889 (s, C≡O), 1593 (w), 1565 (vw), 1486 (w), 1476 (vw), 1451 (w), 1437 (sh), 1378 (w), 1329 (w), 1305 (vw), 1257 (w), 1219 (vw), 1169 (vw), 1062 (w), 1026 (w), 1002 (vw), 995 (vw), 916 (w), 860 (w), 799 (w), 779 (w), 750 cm^{-1} (w); elemental analysis calcd (%) for $C_{16}H_{12}ClN_2O_3Re$: C 38.2, H 2.41, N 5.58; found: C 38.37, H 2.50, N 5.37.

Preparation of ^{ClAr}L: An oven-dried 100 mL Schlenk flask was charged with 4-chloroaniline (1.16 g, 9.09 mmol) and a spatula tip of *p*-toluene sulfonic acid under a dinitrogen atmosphere. Dry benzene (80 mL) and 2-acetylpyridine (1.0 mL, 1.1 g, 9.1 mmol), were added. The reaction solution was then heated to reflux under dinitrogen for 14.5 h and was then allowed to cool to RT. The solvent

was removed under reduced pressure. After the yellow, oily residue had been dried in oil pump vacuum, it was dissolved in Et_2O (10 mL), which was then extracted with three portions of Mili-Q water (5 mL). The organic phase was dried over Na_2SO_4, filtered, and the solvent was removed in vacuum. ^{1}H NMR spectroscopic characterization revealed contamination of the desired product with both of the starting materials. The ligand could be used for the complexation reaction without further purification, however.

Synthesis of ^{ClAr}L-Re: The raw ligand ^{ClAr}**L** (270 mg, max. 1.17 mmol) was dissolved in toluene (4 mL) and combined with $[Re(CO)_5Cl]$ (302 mg, 0.834 mmol) suspended in toluene (10 mL) in a 100 mL Schlenk flask. The reaction mixture was heated to reflux for 16 h under a dinitrogen atmosphere upon which an orange/yellow solid formed. The reaction mixture was allowed to cool to RT to maximize the precipitation. The solvent was decanted and the remaining solid was washed with six portions of Et_2O (2 mL) and dried in vacuum. The product was recrystallized from a THF solution layered with pentane yielding 297 mg (0.554 mmol, 66%) of the analytically pure complex ^{ClAr}**L-Re**. Single crystals suitable for X-ray diffraction were obtained from pentane diffusion into a THF solution. ^{1}H NMR ([D$_8$]THF, 400 MHz): $\delta = 9.07$ (ddd, 1H; $^3J = 5.4$, $^4J = 1.5$, $^5J = 0.7$ Hz, PyH(6)), 8.31 (ddd, 1H; $^3J = 8.0$, $^4J = 1.3$, $^5J = 0.8$ Hz, PyH(3)), 8.23 (ddd, 1H; $^3J = 8.0$, $^3J = 7.7$, $^4J = 1.5$ Hz, PyH(4)), 7.76 (ddd, 1H; $^3J = 7.7$, $^3J = 5.4$, $^4J = 1.4$ Hz, PyH(5)), 7.54 (m, 2H; ArH(3), ArH(5)), 7.44 (m, 1H; ArH(2or6)), 7.10 (m, 1H; ArH(2or6)). 2.46 ppm (s, 3H; $NCCH_3$); ^{13}C{^{1}H} NMR ([D$_8$]THF, 100 MHz): $\delta = 199.6$ (C≡O), 197.5 (C≡O), 188.7 (C≡O), 177.2 ($NCCH_3$), 157.0 (PyC(2)), 154.4 (PyC(6)), 149.6 (ArC(1)), 140.3 (PyC(4)), 133.6 (ArC(4)), 130.7, 130.6 (br, ArC(3), ArC(5), overlapping), 130.0 (PyC(5)), 129.4 (PyC(3)), 124.8 (br, ArC(2or6)), 123.3 (br, ArC(2or6)), 18.4 ppm ($NCCH_3$); IR (THF): $\tilde{\nu} = 2021$ (s, C≡O), 1923 (s, C≡O), 1895 cm^{-1} (s, C≡O); IR (MeCN): $\tilde{\nu} = 2022$ (s, C≡O), 1920 (s, C≡O), 1900 cm^{-1} (s, C≡O); IR (film): $\tilde{\nu} = 2981$ (w), 2870 (w), 2018 (s, C≡O), 1910 (s, C≡O), 1890 (s, C≡O), 1598 (w), 1565 (vw), 1485 (w), 1443 (vw), 1403 (vw), 1378 (w), 1327 (w), 1303 (vw), 1257 (w), 1221 (vw), 1168 (vw), 1091 (w), 1062 (w), 1015 (w), 997 (vw), 913 (vw), 873 (w), 831 (w), 778 (w), 751 (w), 725 cm^{-1} (vw); elemental analysis calcd (%) for $C_{16}H_{11}Cl_2N_2O_3Re$: C 35.83, H 2.07, N 5.22; found: C 36.00, H 2.12, N 5.30.

Preparation of ^{Mes}L: An oven-dried 100 mL Schlenk flask was charged with dry toluene (80 mL), 2-acetylpyridine (1.0 mL, 1.1 g, 9.1 mmol), and 2,4,6-trimethylaniline (1.4 mL, 1.3 g, 9.6 mol) under a dinitrogen atmosphere. A spatula tip of *p*-toluene sulfonic acid was added and the flask was then equipped with a dropping funnel, filled up with dry toluene for the azeotropic removal of water, as well as a reflux condenser. The solution was then heated to reflux under N_2 for 4.5 h. The solution was allowed to cool to RT and the solvent was then removed under reduced pressure. ^{1}H NMR spectroscopic investigation of the remaining yellow oil revealed contamination of the desired product with both of the starting materials. The ligand could be used for the complexation reaction without further purification, however.

Synthesis of ^{Mes}L-Re: The raw ligand ^{Mes}**L** (560 mg, max. 2.35 mmol) was dissolved in toluene (5 mL) and combined with $[Re(CO)_5Cl]$ (465 mg, 1.29 mmol) suspended in toluene (15 mL) in a 100 mL Schlenk flask. The suspension was then heated to reflux for 14 h resulting in an orange/red solution from which an orange solid precipitated upon cooling the solution to 40 °C. The solvent was removed at 40 °C in vacuum and the solid residue was washed in portions with pentane (15 mL) followed by Et_2O (5 mL). The raw product was then recrystallized from pentane diffusion into a THF solution, which led to 562 mg (1.03 mmol; 80%) of ^{Mes}**L-Re** as well as single crystals suitable for X-ray diffraction, which were washed three times with a THF/pentane mixture (1:4, 4 mL) and dried in vacuum. ^{1}H NMR ([D$_8$]THF, 400 MHz): $\delta = 9.07$ (ddd, 1H; $^3J = 5.4$, $^4J = 1.6$, $^5J = 0.8$ Hz, PyH(6)), 8.29 (ddd, 1H; $^3J = 8.0$, $^4J = 1.3$, $^5J = 0.8$ Hz, PyH(3)), 8.23 (ddd, 1H; $^3J = 8.0$, $^3J = 7.7$, $^4J = 1.5$ Hz, PyH(4)), 7.75 (ddd, 1H; $^3J = 7.6$ Hz, $^3J = 5.4$ Hz, $^4J = 1.4$ Hz, PyH(5)), 6.99 (m, 2H; ArH(3), ArH(5)), 2.39 (s, 3H; ArC(2or6)CH_3), 2.34 (s, 3H; $NCCH_3$), 2.32 (s, 3H; ArC(4)CH_3), 2.12 ppm (s, 3H; ArC(2or6)CH_3); ^{13}C{^{1}H} NMR ([D$_8$]THF, 100 MHz): $\delta = 198.7$ (C≡O), 197.9 (C≡O), 189.4 (C≡O), 178.3 ($NCCH_3$), 156.7 (PyC(2)), 154.2 (PyC(6)), 146.5 (ArC(1)), 140.3 (PyC(4)), 137.3 (ArC(4)), 131.2 (ArC(2or6)), 130.3 (ArC(3or5)), 130.7 (ArC(3or5)), 129.8 (PyC(5)), 129.2 (PyC(3)), 128.3 (ArC(2or6)), 21.0 (ArC(4)CH_3), 20.6 (ArC(2or6)CH_3), 18.5 (ArC(2or6)CH_3), 18.3 ppm ($NCCH_3$); IR (THF): $\tilde{\nu} = 2021$ (s, C≡O), 1925 (s, C≡O), 1891 cm^{-1} (s, C≡O); IR (MeCN): $\tilde{\nu} = 2022$ (s, C≡O), 1922 (s, C≡O), 1895 cm^{-1} (s, C≡O); IR (film): $\tilde{\nu} = 2981$ (w), 2924 (w), 2863 (w), 2017 (s, C≡O), 1915 (s, C≡O), 1887 (s, C≡O), 1606 (w), 1590 (w), 1562 (vw), 1475 (w), 1444 (w), 1379 (w), 1329 (w), 1299 (vw), 1256 (w), 1209 (w), 1165 (vw), 1157 (vw), 1119 (vw), 1064 (w), 1028 (vw), 991 (vw), 908 (w), 860 (w), 777 (w), 751 cm^{-1} (w); elemental analysis calcd (%) for $C_{19}H_{18}ClN_2O_3Re$: C 41.95, H 3.34, N 5.15; found: C 42.23, H 3.34, N 5.20.

Synthesis of ^{PrAr}L-Re: The ligand ^{PrAr}**L** (282 mg, 1.01 mmol) was dissolved in toluene (4 mL) and combined with $[Re(CO)_5Cl]$ (270 mg, 0.746 mmol) suspended in toluene (16 mL) in a 100 mL Schlenk flask. The suspension was then heated to reflux for 15 h. After the resulting orange solution was cooled to 40 °C the solvent was removed in vacuum at this temperature. The yellow solid residue was washed in portions with pentane (15 mL) followed by Et_2O (2 mL). The product was then recrystallized from a CH_2Cl_2 solution layered with pentane. This yielded 353 mg (0.602 mmol; 81%) of complex ^{PrAr}**L-Re**, which was washed three times with a mixture of pentane/CH_2Cl_2 (4:1, 5.5 mL) and thoroughly dried in vacuum. Single crystals suitable for X-ray diffraction were obtained from slow diffusion of a concentrated toluene solution at RT. ^{1}H NMR (CD_2Cl_2; 400 MHz): $\delta = 9.07$ (ddd, 1H; $^3J = 5.5$, $^4J = 1.6$, $^5J = 0.8$ Hz, PyH(6)), 8.16 (ddd, 1H; $^3J = 7.9$, $^3J = 7.8$, $^4J = 1.6$ Hz, PyH(4)), 8.09 (ddd, 1H; $^3J = 8.0$, $^4J = 1.4$, $^5J = 0.9$ Hz, PyH(3)), 7.71 (ddd, 1H; $^3J = 7.8$, $^3J = 5.4$, $^4J = 1.5$ Hz, PyH(5)), 7.39–7.31 (m, 3H; ArH(3,4,5)), 3.52 (sept, 1H; $^3J = 6.7$ Hz, $CH(CH_3)_2$), 2.88 (sept, 2H; $^3J = 6.7$ Hz, $CH(CH_3)_2$), 2.37 (s, 3H; $NCCH_3$), 1.34 (d, 3H; $^3J = 6.7$ Hz, $CH(CH_3)_2$), 1.25 (d, 3H; $^3J = 6.6$ Hz, $CH(CH_3)_2$), 1.08 ppm (m, 6H; 2×$CH(CH_3)_2$); ^{13}C{^{1}H} NMR (CD_2Cl_2; 100 MHz): $\delta = 197.6$ (C≡O), 197.3 (C≡O), 188.2 (C≡O), 177.4 ($NCCH_3$), 156.0 (PyC(2)), 153.6 (PyC(6)), 144.8 (ArC(1)), 141.1 (ArC(2 or 6)), 139.8 (PyC(4)), 139.4 (ArC(2 or 6)), 129.4 (PyC(5)), 128.6, 128.4, 125.6, 125.2 (ArC(3,4,5), PyC(3)), 28.6, 28.3 (2×$CH(CH_3)_2$), 25.4, 25.13, 25.07, 24.95 (4×$CH(CH_3)_2$), 20.3 ppm ($NCCH_3$); ^{1}H NMR ([D$_8$]THF, 400 MHz): $\delta = 9.10$ (ddd, 1H; $^3J = 5.4$, $^4J = 1.5$, $^5J = 0.8$ Hz, PyH(6)), 8.30 (ddd, 1H; $^3J = 8.0$, $^4J = 1.6$, $^5J = 0.8$ Hz, PyH(3)), 8.25 (ddd, 1H; $^3J = 8.0$, $^3J = 7.5$, $^4J = 1.5$ Hz, PyH(4)), 7.78 (ddd, 1H; $^3J = 7.5$, $^3J = 5.4$, $^4J = 1.6$ Hz, PyH(5)), 7.35–7.28 (m, 3H; ArH(3,4,5)), 3.71 (sept, 1H; $^3J = 6.7$ Hz, $CH(CH_3)_2$), 2.95 (sept, 2H; $^3J = 6.7$ Hz, $CH(CH_3)_2$), 2.42 (s, 3H; $NCCH_3$), 1.33 (d, 3H; $^3J = 6.7$ Hz, $CH(CH_3)_2$), 1.25 (d, 3H; $^3J = 6.5$ Hz, $CH(CH_3)_2$), 1.07 ppm (m, 6H; 2×$CH(CH_3)_2$); ^{13}C{^{1}H} NMR ([D$_8$]THF, 100 MHz): $\delta = 198.3$ (C≡O), 198.0 (C≡O), 189.0 (C≡O), 178.7 ($NCCH_3$), 156.6 (PyC(2)), 154.2 (PyC(6)), 145.7 (ArC(1)), 141.8 (ArC(2 or 6)), 140.2 (PyC(4)), 140.0 (ArC(2 or 6)), 130.0 (PyC(5)), 129.4 (PyC(3)), 128.8 (ArC(4)), 126.5, 125.4 (ArC(3and5)), 29.0, 28.7 (2×$CH(CH_3)_2$), 25.5, 25.3, 25.2 (3×$CH(CH_3)_2$, overlying with [D8]THF, one hidden), 20.2 ppm ($NCCH_3$); diffusion coefficient ([D$_3$]MeCN, DOSY): $D_0 = 12.7 \times 10^{-10}$ m^{2}s^{-1}; IR (THF): $\tilde{\nu} = 2021$ (s, C≡O), 1925 (s, C≡O), 1893 cm^{-1} (s, C≡O); IR (MeCN): $\tilde{\nu} = 2022$ (s, C≡O), 1922 (s, C≡O), 1897 cm^{-1} (s, C≡O); IR (film): $\tilde{\nu} = 2971$ (w), 2929 (w), 2869 (w), 2017 (s, C≡O), 1914 (s, C≡

O), 1888 (s, C≡O), 1606 (sh), 1594 (w), 1587 (w), 1562 (vw), 1473 (sh), 1464 (w), 1444 (w), 1385 (w), 1375 (w), 1364 (w), 1321 (w), 1257 (w), 1180 (w), 1165 (vw), 1100 (vw), 1065 (w), 1028 (vw), 991 (vw), 936 (vw), 909 (vw), 856 (vw), 809 (vw), 790 (w), 775 (w), 748 (w), 711 cm^{-1} (w); elemental analysis calcd (%) for $C_{22}H_{24}ClN_2O_3Re$: C 45.08, H 4.13, N 4.78; found: C 45.15, H 4.18, N 4.69.

Preparation of ^{MePy}L: In an oven-dried Schlenk flask, 2-acetyl-4-methylpyridine (0.85 mg, 6.3 mmol) was dissolved in dry toluene (60 mL). A spatula tip of *p*-toluene sulfonic acid and aniline (0.80 mL, 0.82 g, 8.8 mmol) were added and the flask was then equipped with a dropping funnel filled with dry toluene. The reaction was then heated to reflux under a dinitrogen atmosphere for 22 h. The reaction mixture was allowed to cool to 40 °C and the solvent was removed in vacuum at this temperature. The obtained yellow residue was further dried in vacuum at 40 °C overnight. Parts of the raw product were dissolved in dry pentane and placed in the freezer at −35 °C for two weeks, which resulted in precipitation of a yellow solid. The solution was decanted and the solid residue was washed three times with small amounts of cold (−35 °C) pentane and dried in vacuum. The product obtained this way was not further isolated and was used for the complexation.

Synthesis of ^{MePy}L-Re: A suspension of $[Re(CO)_5Cl]$ (104 mg, 0.288 mmol) was combined with the raw ligand ^{MePy}L (76 mg, max. 0.361 mmol) in a 100 mL Schlenk flask. The reaction mixture was heated to reflux under a dinitrogen atmosphere for 17 h and was then allowed to cool to 40 °C. The solvent was removed in vacuum at this temperature and the oily residue was then stirred with pentane (15 mL) overnight. The pentane was decanted and the solid residue was washed four times with pentane (2 mL). This procedure was repeated one time, yielding 111 mg (0.215 mmol; 75 %) of the yellow complex ^{MePy}L-Re. Single crystals suitable for X-ray diffraction were obtained from a THF/water mixture. ^{1}H NMR ([D$_8$]THF, 400 MHz): δ = 8.87 (d, 1H; ^3J = 5.5 Hz, PyH(6)), 8.14 (s, 1H; PyH(3)), 7.57 (d, 1H; ^3J = 5.3 Hz, PyH(5)), 7.49 (m, 2H; ArH(3), ArH(5)), 7.43 (m, 1H; ArH(2or6)), 7.31 (m, 1H; ArH(4)), 7.07 (m, 1H; ArH(2or6)), 2.58 (s, 3H; PyC(4)CH_3), 2.41 ppm (s, 3H; NCCH_3); ^4J and ^5J couplings in the pyridine ring could not be reasonably resolved, possibly due to the small additional coupling to the methyl group; ^{13}C{^{1}H} NMR ([D$_8$]THF, 100 MHz): δ = 200.0 (C≡O), 197.6 (C≡O), 189.2 (C≡O), 176.5 (NCCH$_3$), 156.9 (PyC(2)), 153.5 (PyC(6)), 152.9 (PyC(4)), 151.1 (ArC(1)), 130.5 (br, ArC(3and5)), 130.3, 130.2 (PyC(3and5)), 128.1 (ArC(4)), 123.0 (br, ArC(2or6)), 121.4 (br, ArC(2or6)), 21.4 (PyC(4)CH_3), 18.4 ppm (NCCH_3); IR (THF): $\tilde{\nu}$ = 2020 (s, C≡O), 1921 (s, C≡O), 1892 cm^{-1} (s, C≡O); IR (MeCN):$\tilde{\nu}$ = 2021 (s, C≡O), 1918(s, C≡O), 1897 cm^{-1} (s, C≡O); IR (film): $\tilde{\nu}$ = 2981 (w), 2967 (sh), 2869 (w), 2016 (s, C≡O), 1907 (s, C≡O), 1887 (s, C≡O), 1621 (w), 1604 (w), 1593 (w), 1560 (vw), 1486 (w), 1452 (w), 1442 (sh), 1378 (w), 1330 (w), 1304 (vw), 1260 (w), 1224 (w), 1156 (vw), 1088 (sh), 1070 (w), 1030 (w), 1003 (vw), 913 (w), 855 (sh), 834 (w), 775 (w), 741 (w), 699 cm^{-1} (w); elemental analysis calcd (%) for $C_{17}H_{14}ClN_2O_3Re$: C 39.57, H 2.74, N 5.43; found: C 39.94, H 2.86, N 5.64.

Synthesis of ^{PrAr}L-ReTFA: Silver trifluoroacetate (56 mg; 0.25 mmol) was dissolved in THF (3 mL) in an amber vial. To this stirred solution a solution of ^{PrAr}L-Re (59 mg, 0.10 mmol) in THF (2 mL) was added. The reaction mixture was stirred for 2 h in the dark, filtered, and the solvent was removed in vacuum. The solid residue was co-evaporated two times with pentane (2 mL) and then suspended into a mixture of Et_2O/THF (1:1). After filtration and removal of the solvent, the raw product was recrystallized by pentane diffusion into a THF solution, yielding 45 mg (0.068 mmol, 68 %) of complex ^{PrAr}L-ReTFA. Single crystals suitable for X-ray diffraction were obtained from pentane diffusion into a CH_2Cl_2 solution. ^{1}H NMR ([D$_8$]THF, 400 MHz): δ = 9.19 (ddd, 1H; ^3J = 5.4, ^4J = 1.5, ^5J = 0.7 Hz, PyH(6)), 8.35–8.28 (m, 2H; PyH(3,4)), 7.81 (ddd, 1H; ^3J = 7.3, ^3J = 5.3, ^4J = 2.1 Hz, PyH(5)), 7.39–7.30 (m, 3H; ArH(3,4,5)), 3.32 (sept, 1H; ^3J = 6.7 Hz, CH(CH$_3$)$_2$), 2.94 (sept, 2H; ^3J = 6.7 Hz, CH(CH$_3$)$_2$), 2.43 (s, 3H; NCCH$_3$), 1.33 (d, 3H; ^3J = 6.7 Hz, CH(CH_3)$_2$), 1.20 (d, 3H; ^3J = 6.6 Hz, CH(CH_3)$_2$), 1.12 (d, 3H; ^3J = 6.8 Hz, CH(CH_3)$_2$), 1.08 ppm (d, 3H; ^3J = 6.9 Hz, CH(CH_3)$_2$); ^{13}C{^{1}H} NMR ([D$_8$]THF, 100 MHz): δ = 197.6 (C≡O), 196.8 (C≡O), 192.5 (C≡O), 180.3 (NCCH$_3$), 161.2 (q, ^2J = 35.9 Hz, CF_3COO), 156.3 (PyC(2)), 155.6 (PyC(6)), 145.5 (ArC(1)), 141.4 (ArC(2 or 6)), 141.2 (PyC(4)), 139.9 (ArC(2 or 6)), 130.2 (PyC(3)), 129.3 (PyC(5)), 129.0 (ArC(4)), 126.0, 125.7 (ArC(3and5)), 116.7 (q, ^1J = 291.3 Hz, CF_3COO), 29.0, 28.1 (2×CH(CH$_3$)$_2$), 25.4, 25.0, 24.6 (3×CH(CH_3)$_2$, overlying with [D8]THF, one hidden), 19.9 ppm (NCCH_3); ^{19}F NMR ([D$_8$]THF, 376 MHz): δ = −74.0 ppm (CF_3COO); diffusion coefficient ([D$_3$]MeCN, DOSY): $D_0 = 13.0\times10^{-10}$ m^2s^{-1}; IR (THF): $\tilde{\nu}$ = 2026 (s, C≡O), 1936 (s, C≡O), 1903 (s, C≡O), 1716 (w, C=O (TFA)), 1701 cm^{-1} (w, C=O (TFA)); IR (MeCN): $\tilde{\nu}$ = 2026 (s, C≡O), 1924 (s, C≡O), 1905 (s, C≡O), 1717 (w, C=O (TFA)), 1700 cm^{-1} (w, C=O (TFA)); IR (film): $\tilde{\nu}$ = 2970 (w), 2932 (w), 2871 (w), 2021 (s, C≡O), 1916 (s, C≡O), 1894 (s, C≡O), 1714 (sh, C=O), 1695 (m, C=O), 1607 (sh), 1594 (w), 1588(w), 1565 (vw), 1466 (w), 1446 (w), 1410 (w, C–O), 1387 (w), 1376 (w), 1365 (w), 1322 (w), 1258 (w), 1191 (s, asym. CF_3), 1140 (m, sym. CF_3), 1104 (vw), 1064 (w), 1029 (vw), 991 (vw), 936 (vw), 908 (vw), 844 (w), 809 (vw), 790 (w), 776 (w), 749 (w), 726 (m), 712 cm^{-1} (vw); elemental analysis calcd (%) for $C_{24}H_{24}F_3N_2O_5Re$: C 43.44, H 3.65, N 4.22; found: C 43.47, H 3.61, N 4.22.

Synthesis of [^{Mes}L-Re]$_2$: A solution of ^{Mes}L-Re (32 mg, 59 μmol) in THF (4 mL) and KC_8 (9 mg, 67 μmol) were separately cooled to −35 °C. The cold complex solution was then added to the cold KC_8 and the resulting suspension was stirred for 15 min while warming up before the reaction mixture was filtered. The resulting solution was reduced to 1 mL and layered with pentane. Green and orange crystals grew from this mixture at −35 °C, which were washed three times with a mixture of THF/pentane (1:4, 1 mL) and dried in vacuum. The unreduced, orange starting material was removed by extracting with two time 0.2 mL of MeCN, resulting in 7 mg (6.9 μmol, 23 %) of the green complex [^{Mes}L-Re]$_2$. Single crystals suitable for X-ray diffraction were obtained from pentane diffusion into a toluene solution at −35 °C. ^{1}H NMR ([D$_8$]THF, 400 MHz): δ = 8.33 (ddd, 1H; ^3J = 8.4, ^4J = 1.4, ^5J = 1.9 Hz, PyH(3)), 7.61 (ddd, 1H; ^3J = 8.5, ^3J = 7.1 ^4J = 1.5 Hz, PyH(4)), 7.17 (ddd, 1H; ^3J = 7.1, ^3J = 5.8, ^4J = 1.4 Hz, PyH(5)), 6.94, 6.90 (m, 2H; ArH(3), ArH(5)), 6.21 (ddd, 1H; ^3J = 5.9, ^4J = 1.4, ^5J = 1.0 Hz, PyH(6)), 2.51 (s, 3H; NCCH$_3$), 2.30 (s, 3H; ArC(4)CH$_3$), 2.08 (s, 3H; ArC(2or6)CH$_3$), 1.97 ppm (s, 3H; ArC(2or6)CH$_3$); ^{13}C{^{1}H} NMR ([D$_8$]THF, 100 MHz): δ = 203.2 (C≡O), 200.6 (C≡O), 190.1 (C≡O), 159.1 (NCCH$_3$), 151.8 (PyC(6)), 150.1 (PyC(2)), 149.1 (ArC(1)), 136.0 (ArC(4)), 131.0, 130.0, 129.9, 129.72, 129.66 (ArC(2), ArC(3), ArC(5), ArC(6), PyC(4)), 127.9 (PyC(3)), 120.6 (PyC(5)), 21.0 (ArC(4)CH_3), 20.3 (ArC(2or6)CH_3), 18.7 (ArC(2or6)CH_3), 17.5 ppm (NCCH_3); IR (THF): $\tilde{\nu}$ = 1991 (s, C≡O), 1962 (s, C≡O), 1902 (m, C≡O), 1885 (s, C≡O), 1862 cm^{-1} (m, C≡O); IR (film): $\tilde{\nu}$ = 2984 (w), 2922 (w), 2859 (w), 1986 (m, C≡O), 1955 (s, C≡O), 1898 (m, C≡O), 1875 (s, C≡O), 1861 (sh, C≡O), 1595 (w), 1540 (vw), 1486 (w), 1457 (w), 1437 (w), 1401 (m), 1381 (w), 1343 (m), 1254 (m), 1209 (w), 1157 (w), 1082 (w), 1067 (vw), 1013 (vw), 996 (m), 982 (w), 953 (vw), 859 (vw), 761 (w), 735 cm^{-1} (w); elemental analysis calcd (%) for $C_{38}H_{36}N_4O_6Re_2$: C 44.87, H 3.57, N 5.51; found: C 44.64, H 3.60, N 5.53.

Preparation of ^{Ph}L-Re$^-$: The complex ^{Ph}L-Re (13 mg, 26 μmol) was dissolved in THF (4 mL) and the solution was added to freshly prepared Na/Hg (18 mg, 0.78 mmol, Na in 2.646 g Hg) upon which the color of the solution quickly turned green. The mixture was stirred for one hour and became deep red after this time. The solution

was decanted from the amalgam, filtered, and the solvent was removed in vacuum. The complex ^{Ph}**L-Re$^-$** was not isolated in this study but spectroscopically characterized. ^{1}H NMR ([D$_8$]THF, 400 MHz): δ = 8.59 (ddd, 1H; ^3J = 6.7, ^4J = 1.2, ^5J = 1.2 Hz, PyH(6)), 7.12 (dd, 2H; ^3J = 8.2, ^3J = 7.3 Hz, ArH(3,5)), 7.01 (dd, 2H; ^3J = 8.2, ^4J = 1.2 Hz, ArH(2,6)), 6.91 (tt, 1H; ^3J = 7.3, ^4J = 1.2 Hz, ArH(4)), 6.64 (ddd, 1H; ^3J = 9.2, ^4J = 1.2, ^5J = 1.2 Hz, PyH(3)), 5.92 (ddd, 1H; ^3J = 9.2, ^3J = 5.9, ^4J = 1.1 Hz, PyH(4)), 4.96 (ddd, 1H; ^3J = 6.7, ^3J = 5.9, ^4J = 1.3 Hz, PyH(5)), 1.96 ppm (s, 3H; NCCH_3); ^{13}C{^{1}H} NMR ([D$_8$]THF, 100 MHz): δ = 211.6 (C≡O), 158.9 (ArC(1)), 153.8 (PyC(6)), 136.5 (PyC(2)), 127.9 (ArC(3,5)), 127.2 (ArC(2,6)), 123.4 (NCCH$_3$), 123.3 (ArC(4)), 122.5 (PyC(3)), 118.4 (PyC(4)), 102.7 (PyC(5)) and 14.7 ppm (NCCH_3); IR (THF): $\tilde{\nu}$ = 1954 (s, C≡O), 1851 (s, C≡O), 1810 cm^{-1} (s, C≡O).

Preparation of ^{PrAr}L-Re$^-$: The chlorido complex ^{PrAr}**L-Re** (45 mg; 0.077 mmol) was dissolved in THF (3 mL) and this solution was added to sodium (96 mg, 4.2 mmol) dissolved in Hg (14 g). The reaction mixture was stirred for 14.5 h and filtered. The solvent was then removed in vacuum and the residue was co-evaporated with pentane (2 mL) and dried in vacuum. NMR spectroscopic characterization indicated the clean formation of the complex ^{PrAr}**L-Re$^-$**. Single crystals suitable for X-ray diffraction and the analytically pure complex were obtained from a diluted pentane solution, which contained traces of THF (≈10:1) at −35 °C, yielding 38 mg (0.041 mmol; 53%) of the complex ^{PrAr}**L-Re$^-$·5 THF**. Although the asymmetric unit of the crystal structure contains five molecules of THF per complex molecule, elemental analysis of the crystalline material after excessive drying in vacuum indicated complete loss of these solvent molecules. ^{1}H NMR ([D$_8$]THF, 400 MHz): δ = 8.61 (ddd, 1H; ^3J = 6.7, ^4J = 1.2, ^5J = 1.2 Hz, PyH(6)), 7.04–6.93 (m, 3H; ArH(3,4,5)), 6.67 (ddd, 1H; ^3J = 9.3, ^4J = 1.2, ^5J = 1.2 Hz, PyH(3)), 5.93 (ddd, 1H; ^3J = 9.3, ^3J = 5.9, ^4J = 1.1 Hz, PyH(4)), 4.99 (ddd, 1H; ^3J = 6.9, ^3J = 5.9, ^4J = 1.1 Hz, PyH(5)), 2.72 (sept, 2H; ^3J = 6.9 Hz, CH(CH$_3$)$_2$), 1.83 (s, 3H; NCCH_3), 1.15 (d, 3H; ^3J = 6.8 Hz, CH(CH_3)$_2$), 1.01 ppm (d, 3H; ^3J = 7.0 Hz, CH(CH_3)$_2$); ^{13}C{^{1}H} NMR ([D$_8$]THF, 100 MHz): δ = 211.6 (C≡O), 154.2 (PyC(6)), 153.4 (ArC(1)), 136.7 (PyC(2)), 142.7 (ArC(2,6)), 124.7 (ArC(4)), 122.6 (NCCH$_3$), 122.5 (ArC(3,5)), 122.3 (PyC(3)), 118.4 (PyC(4)), 102.3 (PyC(5)), 27.7 (CH(CH$_3$)$_2$), 25.9, 24.3 (2×CH(CH_3)$_2$), 14.4 ppm (NCCH_3); IR (MeCN): $\tilde{\nu}$ = 1951 (s, C≡O), 1844 (s, C≡O), 1835 cm^{-1} (s, C≡O); IR (THF): $\tilde{\nu}$ = 1952 (s, C≡O), 1851 (s, C≡O), 1810 cm^{-1} (s, C≡O); elemental analysis calcd (%) for $C_{22}H_{24}N_2NaO_3Re$: C 46.06, H 4.22, N 4.88; found: C 45.26, H 4.55, N 4.97.

Acknowledgements

This material is based upon work performed by the Joint Center for Artificial Photosynthesis, a DOE Energy Innovation Hub, supported through the Office of Science of the U.S. Department of Energy under Award Number DE-SC0004993. Michael Takase, Lawrence M. Henling and David G. VanderVelde are thanked for their invaluable work in the X-ray (M.T. and L.M.H.) and NMR (D.G.V.V) facilities at Caltech and a lot of helpful discussions. The authors are indebted to Natascha Junker, Bernhard E. C. Bugenhagen, and especially Prof. Peter Burger for help with the DFT calculations and generous computation time on the IAAC cluster at the University of Hamburg.

Keywords: alpha diimines · NMR spectroscopy · redox-active ligands · rhenium · X-ray crystallography

[1] C. K. Jørgensen, *Coord. Chem. Rev.* **1966**, *1*, 164–178.
[2] a) J. A. McCleverty, *Chem. Rev.* **2004**, *104*, 403–418; b) D. Steinborn, *J. Chem. Educ.* **2004**, *81*, 1148; c) V. K. Landry, K. Pang, S. M. Quan, G. Parkin, *Dalton Trans.* **2007**, 820–824; d) W. J. Evans, M. Fang, J. E. Bates, F. Furche, J. W. Ziller, M. D. Kiesz, J. I. Zink, *Nat. Chem.* **2010**, *2*, 644–647.
[3] W. Kaim, *Eur. J. Inorg. Chem.* **2012**, 343–348.
[4] a) J. I. van der Vlugt, *Eur. J. Inorg. Chem.* **2012**, 363–375; b) K. G. Caulton, *Eur. J. Inorg. Chem.* **2012**, 435–443; c) R. Eisenberg, H. B. Gray, *Inorg. Chem.* **2011**, *50*, 9741–9751; d) W. Kaim, *Inorg. Chem.* **2011**, *50*, 9752–9765; e) W. I. Dzik, X. P. Zhang, B. de Bruin, *Inorg. Chem.* **2011**, *50*, 9896–9903; f) V. Lyaskovskyy, B. de Bruin, *ACS Catal.* **2012**, *2*, 270–279; g) O. R. Luca, R. H. Crabtree, *Chem. Soc. Rev.* **2013**, *42*, 1440–1459; h) W. Kaim, B. Schwederski, *Coord. Chem. Rev.* **2010**, *254*, 1580–1588.
[5] a) P. Clopath, A. von Zelewsky, *J. Chem. Soc. D* **1971**, 47b; b) S. Richter, C. Daul, A. von Zelewsky, *Inorg. Chem.* **1976**, *15*, 943–948; c) M. H. Chisholm, J. C. Huffman, I. P. Rothwell, P. G. Bradley, N. Kress, W. H. Woodruff, *J. Am. Chem. Soc.* **1981**, *103*, 4945–4947; d) G. van Koten, K. Vrieze in *Advances in Organometallic Chemistry* (Eds.: F. G. A. Stone, R. West), Academic Press, New York, **1982**, pp. 151–239; e) E. Uhlig, *Pure Appl. Chem.* **1988**, *60*, 1235–1240; f) W. Kaim, R. Reinhardt, M. Sieger, *Inorg. Chem.* **1994**, *33*, 4453–4459; g) D. Zhu, P. H. M. Budzelaar, *Organometallics* **2008**, *27*, 2699–2705; h) W. Kaim, M. Sieger, S. Greulich, B. Sarkar, J. Fiedler, S. Zálišý, 12th International Symposium on Inorganic Ring Systems (IRIS 12), **2010**, *695*, 1052–1058; i) C. C. Scarborough, K. Wieghardt, *Inorg. Chem.* **2011**, *50*, 9773–9793; j) V. C. Gibson, C. Redshaw, G. A. Solan, *Chem. Rev.* **2007**, *107*, 1745–1776.
[6] P. H. M. Budzelaar, B. Bruin, A. W. Gal, K. Wieghardt, J. H. van Lenthe, *Inorg. Chem.* **2001**, *40*, 4649–4655.
[7] Q. Knijnenburg, D. Hetterscheid, T. M. Kooistra, P. H. M. Budzelaar, *Eur. J. Inorg. Chem.* **2004**, 1204–1211.
[8] Q. Knijnenburg, S. Gambarotta, P. H. M. Budzelaar, *Dalton Trans.* **2006**, 5442–5448.
[9] a) J. Hawecker, J.-M. Lehn, R. Ziessel, *J. Chem. Soc. Chem. Commun.* **1984**, 328–330; b) J. Hawecker, J.-M. Lehn, R. Ziessel, *J. Chem. Soc. Chem. Commun.* **1983**, 536–538.
[10] J. Hawecker, J.-M. Lehn, R. Ziessel, *Helv. Chim. Acta* **1986**, *69*, 1990–2012.
[11] B. P. Sullivan, C. M. Bolinger, D. Conrad, W. J. Vining, T. J. Meyer, *J. Chem. Soc. Chem. Commun.* **1985**, 1414–1416.
[12] a) P. Christensen, A. Hamnett, A. V. G. Muir, J. A. Timney, *J. Chem. Soc. Dalton Trans.* **1992**, 1455–1463; b) K. A. Grice, N. X. Gu, M. D. Sampson, C. P. Kubiak, *Dalton Trans.* **2013**, *42*, 8498–8503; c) M. D. Sampson, J. D. Froehlich, J. M. Smieja, E. E. Benson, I. D. Sharp, C. P. Kubiak, *Energy Environ. Sci.* **2013**, *6*, 3748–3755; d) K. A. Grice, C. P. Kubiak in *Advances in Inorganic Chemistry: CO_2 Chemistry* (Eds.: M. Aresta, R. van Eldik), Academic Press, New York, **2014**, pp. 163–188; e) M. D. Sampson, A. D. Nguyen, K. A. Grice, C. E. Moore, A. L. Rheingold, C. P. Kubiak, *J. Am. Chem. Soc.* **2014**, *136*, 5460–5471.
[13] F. P. A. Johnson, M. W. George, F. Hartl, J. J. Turner, *Organometallics* **1996**, *15*, 3374–3387.
[14] J. M. Smieja, E. E. Benson, B. Kumar, K. A. Grice, C. S. Seu, A. J. M. Miller, J. M. Mayer, C. P. Kubiak, *Proc. Natl. Acad. Sci. USA* **2012**, *109*, 15646–15650.
[15] E. E. Benson, M. D. Sampson, K. A. Grice, J. M. Smieja, J. D. Froehlich, D. Friebel, J. A. Keith, E. A. Carter, A. Nilsson, C. P. Kubiak, *Angew. Chem. Int. Ed.* **2013**, *52*, 4841–4844; *Angew. Chem.* **2013**, *125*, 4941–4944.
[16] G. J. Stor, F. Hartl, J. W. M. van Outersterp, D. J. Stufkens, *Organometallics* **1995**, *14*, 1115–1131.
[17] J. M. Smieja, C. P. Kubiak, *Inorg. Chem.* **2010**, *49*, 9283–9289.
[18] E. E. Benson, K. A. Grice, J. M. Smieja, C. P. Kubiak, *Polyhedron* **2013**, *58*, 229–234.
[19] a) J. Agarwal, T. W. Shaw, C. J. Stanton, G. F. Majetich, A. B. Bocarsly, H. F. Schaefer, *Angew. Chem. Int. Ed.* **2014**, *53*, 12253; *Angew. Chem.* **2014**, *126*, 5252–5255; b) Q. Zeng, J. Tory, F. Hartl, *Organometallics* **2014**, *33*, 5002–5008; c) M. V. Vollmer, C. W. Machan, M. L. Clark, W. E. Antholine, J. Agarwal, H. F. Schaefer III, C. P. Kubiak, J. R. Walensky, *Organometallics* **2015**, *34*, 3–12.
[20] D. Sieh, D. C. Lacy, J. C. Peters, C. P. Kubiak, *Chem. Eur. J.* **2015**, *21*, 8497–8503.
[21] M. H. B. Stiddard, *J. Chem. Soc.* **1962**, 4712–4715.

[22] a) A. G. Robietti, J. Thompson, *Spectrochim. Acta* **1965**, *21*, 2023 – 2030; b) P. C. Angus, S. R. Stobart, *J. Chem. Soc. Dalton Trans.* **1975**, 2342 – 2347.
[23] B. de Bruin, E. Bill, E. Bothe, T. Weyhermüller, K. Wieghardt, *Inorg. Chem.* **2000**, *39*, 2936 – 2947.
[24] C. C. Lu, E. Bill, T. Weyhermüller, E. Bothe, K. Wieghardt, *J. Am. Chem. Soc.* **2008**, *130*, 3181 – 3197.
[25] C. C. Lu, T. Weyhermüller, E. Bill, K. Wieghardt, *Inorg. Chem.* **2009**, *48*, 6055 – 6064.
[26] a) M. van Gastel, C. C. Lu, K. Wieghardt, W. Lubitz, *Inorg. Chem.* **2009**, *48*, 2626 – 2632; b) T. W. Myers, G. M. Yee, L. A. Berben, *Eur. J. Inorg. Chem.* **2013**, 3831 – 3835.
[27] T. W. Myers, N. Kazem, S. Stoll, R. D. Britt, M. Shanmugam, L. A. Berben, *J. Am. Chem. Soc.* **2011**, *133*, 8662 – 8672.
[28] H. P. Nayek, N. Arleth, I. Trapp, M. Löble, P. Oña-Burgos, M. Kuzdrowska, Y. Lan, A. K. Powell, F. Breher, P. W. Roesky, *Chem. Eur. J.* **2011**, *17*, 10814 – 10819.
[29] K. Nienkemper, V. V. Kotov, G. Kehr, G. Erker, R. Fröhlich, *Eur. J. Inorg. Chem.* **2006**, 366 – 379.
[30] D. Sieh, M. Schlimm, L. Andernach, F. Angersbach, S. Nückel, J. Schöffel, N. Šušnjar, P. Burger, *Eur. J. Inorg. Chem.* **2012**, 444 – 462.
[31] C. Tejel, M. P. del Río, M. A. Ciriano, E. J. Reijerse, F. Hartl, S. Záliš, D. G. H. Hetterscheid, N. Tsichlis i Spithas, B. de Bruin, *Chem. Eur. J.* **2009**, *15*, 11878 – 11889.
[32] a) C. Tejel, M. A. Ciriano, M. P. del Río, D. G. H. Hetterscheid, N. Tsichlis i Spithas, J. M. M. Smits, B. de Bruin, *Chem. Eur. J.* **2008**, *14*, 10932 – 10936; b) C. Tejel, L. Asensio, M. Pilar del Río, B. de Bruin, J. A. López, M. A. Ciriano, *Eur. J. Inorg. Chem.* **2012**, 512 – 519.
[33] L. J. Todd, J. R. Wilkinson, J. P. Hickey, D. L. Beach, K. W. Barnett, *J. Organomet. Chem.* **1978**, *154*, 151 – 157.
[34] P. C. Lauterbur, R. B. King, *J. Am. Chem. Soc.* **1965**, *87*, 3266 – 3267.
[35] P. C. Servaas, G. J. Stor, D. J. Stufkens, A. Oskam, *Inorg. Chim. Acta* **1990**, *178*, 185 – 194.
[36] E. Fujita, J. T. Muckerman, *Inorg. Chem.* **2004**, *43*, 7636 – 7647.
[37] At these high dilutions partial formation of the THF complex ^{Mes}L-Re(THF) seems very likely, therefore, the extinction coefficients given here are rather an estimation.
[38] E. E. Benson, C. P. Kubiak, *Chem. Commun.* **2012**, *48*, 7374 – 7376.
[39] J. Reinhold, R. Benedix, P. Birner, H. Hennig, *Inorg. Chim. Acta* **1979**, *33*, 209 – 213.
[40] M. Kriechbaum, D. Otte, M. List, U. Monkowius, *Dalton Trans.* **2014**, *43*, 8781 – 8791.
[41] Y.-W. Dong, R.-Q. Fan, P. Wang, Y.-L. Yang, *Acta Crystallogr. Sect. A* **2012**, *68*, o1427.
[42] L. H. Polm, G. van Koten, C. J. Elsevier, K. Vrieze, B. F. K. van Santen, C. H. Stam, *J. Organomet. Chem.* **1986**, *304*, 353 – 370.
[43] Y. Li, K. C. Mondal, P. Stollberg, H. Zhu, H. W. Roesky, R. Herbst-Irmer, D. Stalke, H. Fliegl, *Chem. Commun.* **2014**, *50*, 3356 – 3358.
[44] R. J. Baker, C. Jones, M. Kloth, D. P. Mills, *New J. Chem.* **2004**, *28*, 207 – 213.
[45] G. van Koten, J. T. B. H. Jastrzebski, K. Vrieze, *J. Organomet. Chem.* **1983**, *250*, 49 – 61.
[46] The model ligand ^{mod}**L** has a 2,6-dimethylaryl substituent. See the Supporting Information.
[47] a) J. W. M. van Outersterp, F. Hartl, D. J. Stufkens, *Organometallics* **1995**, *14*, 3303 – 3310; b) Y. Hayashi, S. Kita, B. S. Brunschwig, E. Fujita, *J. Am. Chem. Soc.* **2003**, *125*, 11976 – 11987. See also Ref. [12b].
[48] Although the asymmetric unit of the crystalline material contains five THF molecules, elemental analysis of the isolated complex ^{PrAr}**L-Re**$^{-}$ indicates that the THF molecules can be removed by extensive drying in oil pump vacuum.
[49] F. H. Allen, O. Kennard, D. G. Watson, L. Brammer, A. G. Orpen, R. Taylor, *J. Chem. Soc. Perkin Trans. 2* **1987**, S1 – S19.
[50] T. W. Myers, L. A. Berben, *J. Am. Chem. Soc.* **2011**, *133*, 11865 – 11867.
[51] T. V. Laine, U. Piironen, K. Lappalainen, M. Klinga, E. Aitola, M. Leskelä, *J. Organomet. Chem.* **2000**, *606*, 112 – 124.
[52] D. Savoia, C. Trombini, A. Umani-Ronchi, *Pure Appl. Chem.* **1985**, *57*, 1887 – 1896.
[53] SAINT, 1997 – 2013, Bruker AXS Inc., Madison, WI, **2013**.
[54] G. M. Sheldrick, SADABS, Bruker AXS Inc., Madison, WI, **2012**.
[55] G. M. Sheldrick, *Acta Crystallogr. Sect. A* **2008**, *64*, 112 – 122.
[56] A. Altomare, M. C. Burla, M. Camalli, G. L. Cascarano, C. Giacovazzo, A. Guagliardi, A. G. G. Moliterni, G. Polidori, R. Spagna, *J. Appl. Crystallogr.* **1999**, *32*, 115 – 119.
[57] C. B. Hübschle, G. M. Sheldrick, B. Dittrich, *J. Appl. Crystallogr.* **2011**, *44*, 1281 – 1284.

Received: February 14, 2016
Published online on ■■ ▮▮, 0000

FULL PAPER

Rhenium Complexes

*D. Sieh, C. P. Kubiak**

■■ – ■■

A Series of Diamagnetic Pyridine Monoimine Rhenium Complexes with Different Degrees of Metal-to-Ligand Charge Transfer: Correlating ^{13}C NMR Chemical Shifts with Bond Lengths in Redox-Active Ligands

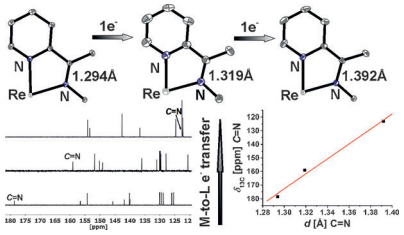

Linear correlation: A series of diamagnetic pyridine monoimine rhenium complexes with different degrees of metal-to-ligand charge transfer was investigated by ^{13}C NMR spectroscopy and single-crystal X-ray diffraction and linear correlations were observed correlating relevant bond length with the carbon NMR shifts of the respective carbon atoms.